Satellite Based Estimated of Global Precipitation Water and Poleward Latent Heat Transport

by
Ian L. Wittmeyer

Department of Atmospheric Science
Colorado State University
Fort Collins, Colorado

Colorado State University

Department of Atmospheric Science

Paper No. 473

SATELLITE BASED ESTIMATES OF GLOBAL PRECIPITABLE WATER AND POLEWARD LATENT HEAT TRANSPORT

by

Ian L. Wittmeyer

Research supported by NASA Grant NAG 1-865

Principal Investigator: Thomas H. Vonder Haar

Fall, 1990

Atmospheric Science Paper No. 473

This paper was also submitted in partial fulfillment of the
requirements for the degree of Masters of Science.

ABSTRACT

SATELLITE BASED ESTIMATES OF GLOBAL PRECIPITABLE WATER DISTRIBUTION AND POLEWARD LATENT HEAT FLUX

Recent availability of long term global satellite observations of precipitable water allows for new estimates of the role of moisture in our climate. Moisture transport is the least known component of all poleward fluxes due to the highly variable nature of moisture in the atmosphere. The present study uses a five year precipitable water data set retrieved by satellite based TIROS Operational Vertical Sounder (TOVS) instruments. Large scale precipitable water content properties are well illustrated by the International Satellite Cloud Climatology Project (ISCCP) version of the TOVS data. Some synoptic scale features are often not well represented in the data due to inherent restrictions within the TOVS retrieval scheme. Daily global coverage allows polar orbiting sensors to sense the atmosphere in very different ways than from ground based systems. Wind analyses from the European Center for Medium Range Weather Forecasts are used along with the TOVS data in the calculation of poleward moisture transport.

Poleward atmospheric latent heat transport plays an important role in moving energy from the tropics to high latitudes. Up to half of the peak meridional atmospheric heat flux, estimated at near 4 PW, can be attributed to the latent energy term. This moist energy component is less well known than the other contributing components, namely the sensible heat and potential energy terms. Three separate components comprise the total moisture transport, and their relative contributions vary with latitude. The total transport in midlatitudes and the subtropics is dominated by transient and standing eddy terms (near 25 and 40 degrees latitude respectively) where peak values are generally less

than 0.5 PW in the annual mean. Mean meridional circulation is most important in tropical latitudes where peak values exceed 4 PW during many months of a given year. Monthly mean zonal transport of latent heat is maximized in the tropics, with peaks near 5 PW, while midlatitude values are much smaller (generally less than 1.0 PW). Data biases are obvious in the midlatitude values, where peak transports are presumed to closer to 2 PW. Peak monthly midlatitude eddy transport occurs in April, and also in the fall, during seasonal transition periods. Annual midlatitude transports are fairly similar to those during any given month of the year. Conversely, tropical transports show large seasonal variations, and therefore annual values reflect some cancellation due to this periodic nature. Climatological mean moisture distribution and transport analyses suffer from a number of factors which prevent any clear sign of interannual variation. Special analyses of presently available data sets are needed to more clearly characterize the role of moisture in climate. In addition, new data sets are critically needed to adequately detail the important smaller scale features which significantly contribute to large scale climatological conditions.

ACKNOWLEDGEMENTS

A number of people provided a wide range of support during this study, and to them I am grateful. Professor Vonder Haar provided an excellent environment for a successful learning experience, and his advice and guidance proved very useful. I acknowledge Garrett Campbell of the Cooperative Institute for Research in the Atmosphere (CIRA) and Roy Jenne of NCAR (which is sponsored by the National Science Foundation) for acquisition of a whole library of ECMWF analysis tapes. ECMWF itself was especially kind to send a number of hard-to-find publications which described their operational model, its analyses, and archives. Lola Olson of the National Space Science Data Center provided the needed ISCCP TOVS data tapes, and adequate documentation thereof. All calculations were performed using CIRA computing facilities here at CSU.

Support within our group has been fantastic. Dave Randel provided a number of software routines for various applications ranging from data tape unpacking to output display. Kelly Dean installed and maintained additional display software which I used extensively. Drafted graphics were skillfully performed by Judy Sorbie-Dunn. Loretta Wilson, Joanne DiVico, and Lisa Huss-Dattore assisted me in a variety of tasks. Finally, I would like to thank my wife, Kelley, for her undying support and encouragement.

This work has been supported by NASA grant NAG 1-865.

TABLE OF CONTENTS

LIST OF TABLES

LIST OF FIGURES

Chapter 1

INTRODUCTION

The study of large scale atmospheric moisture content and its transport on the large scale is relatively new. While early theories of atmospheric circulation date back to the eighteenth century (see Lorenz (1967) for a discussion of the history of general circulation theories), only recently have we been able to measure atmospheric variables to verify these ideas. The establishment of a synoptic network of upper air monitoring systems was key in providing enough data for adequate characterization of the mean state of the atmosphere. Ideas put forth by researchers such as Hadley, Dove, Ferrel, and many later investigators, could then be tested and verified using physical *in situ* data.

The characterization of large scale moisture fields was advanced by Bannon and Steele (1960), who used multi-year data from the newly established post-World War II radiosonde network. The first moisture climatology showed significant structure over land where there were observations, and smoothed patterns over the oceans where data filling was necessary. An early moisture transport study by Benton and Estoque (1954) characterized seasonal and annual fluxes of water vapor over North America, showed the importance of atmospheric eddies in meridional water vapor transport, and estimated the water balance of this region. Starr, Peixoto, and Lividas (1958) used data from 1950 to describe the seasonal and annual means of precipitable water and poleward water vapor transport in the Northern Hemisphere. A summary of early moisture transport, water balance, and precipitation minus evaporation calculations is given in Sellers (1965).

The abundance of data during the 1958 International Geophysical Year (IGY) provided for a more accurate assessment of large scale atmospheric moisture conditions. Starr, Peixoto, and Crisi (1965) described the Northern Hemisphere water balance and transport

for the IGY. A detailed study by Starr, Peixoto, and McKean (1969) used this data set to investigate the global distribution of water content and its flux divergence. Also presented are estimates of evaporation minus precipitation as compared with other early independent estimates. Rasmusson (1966) used twice daily radiosonde information for the summer of 1958 to characterize diurnal variations in moisture transport over North America. He found substantial differences in 1200 GMT water vapor transport as compared with 0000 GMT data for the summer months studied.

The expanding synoptic upper air network during the 1960's and 1970's allowed for improved multi-year data sets to be used in climate research. A number of studies used data from the General Circulation Data Library at the Massachusetts Institute of Technology (MIT), which contains analyses of worldwide radiosonde observations from 1958 to 1963 (see Starr *et al.*, 1970). The annual cycle of poleward energy transport was investigated by Oort (1971). Results showed the importance of atmospheric eddies in the annual poleward transport of energy. The tropical Hadley cell circulation is strong in any particular month, but contributes less to the total annual mean energy transport due to cancellation of the large seasonal fluctuations. In addition, peak atmospheric energy transports were shown to occur in November and April during seasonal transition periods.

Rosen *et al.* (1979), and Peixoto *et al.* (1981), examined variations in large scale moisture for interannual, and intra-annual periods, respectively. New estimates of poleward water vapor transport, net precipitation minus evaporation, and precipitable water distribution are given. The multi-year study shows little variation in the zonally averaged atmospheric water content, and highlights significant variation in the interannual moisture transport. This is especially true when data separated by a number of years is used, or where two significantly different global atmospheric circulation patterns exist. Oort (1985) used fifteen years of general circulation data to present a complete set of atmospheric statistics for a large number of variables, including transport of moisture.

Recent moisture transport studies have verified, and expanded upon, the early findings. Using a data set produced by the Geophysical Fluid Dynamics Laboratory of the First Global GARP Experiment (FGGE) level III-b analyses of atmospheric data, Chen

(1985) investigated moisture content and transport quantities (GARP is the Global Atmospheric Research Program). Reaffirming Oort (1971), Chen's results show the importance of the Hadley and Walker circulations for the concentration of water vapor maxima at tropical latitudes, and the importance of standing and transient eddies in moving moisture poleward. The lack of agreement at midlatitudes signifies the difficulty in properly assessing the eddy terms, which dominate the total transport. Oort (1977) cautions the use of data from the present radiosonde network in general circulation studies on subsynoptic space scales. This would imply the inadequacy of present ground based systems to "see" the entire structure of the moisture field especially at smaller, more important scales. Mean quantities are accurate while eddy terms tend to be less well known. Use of additional information, such as satellite data, can enhance ground based data sets and provide for better estimates of certain atmospheric quantities.

Satellite data can be used in both a direct, and indirect calculation of atmospheric heat transport. The indirect calculation of ocean and atmosphere transports using satellite data was pioneered by Vonder Haar and Oort (1973). The annual net radiation at the top of the atmosphere balances oceanic and atmospheric heat transports in a polar cap, assuming negligible storage in the annual mean. Therefore, using an independent source of one transport quantity allows for the indirect estimate of the other. Later works by Oort and Vonder Haar (1976), Carissimo *et al.* (1985), and Kann *et al.* (1990) employed this technique, and results of derived atmospheric heat transport agree favorably with independent, ground based values.

Direct estimates of atmospheric latent heat transport, as shown in Masuda (1988), show agreement among three independent sources for the total flux, while individual components of the total transport are represented with more uncertainty. Differences on the order of one petawatt are common in seasonal transport, for individual components, and the uncertainty accounts for a substantial percent of the total values. Agreement is poorest in the midlatitudes where eddy terms dominate.

The present study uses satellite precipitable water measurements, along with model analysis fields, in a direct calculation of atmospheric moisture, and latent heat transport.

A large degree of uncertainty exists in present estimates of these quantities and, therefore, recent long term data sets are used to address the problem. While these new global data sets provide valuable new insight into atmospheric components of Earth's hydrologic cycle, they fall short in revealing answers to some of the most pressing climate questions. Interannual variability of global moisture and transport does not yet exceed the data noise level and important high frequency features are not well represented. Mean state properties are adequately described while transient features, such as atmospheric eddies, are not. However, knowledge of biases and other errors aids in our further understanding of this subject.

The present study specifically addresses the method, theory, analysis and discussion of moisture distribution and flux. The following chapter gives an outline of the applicable method and theory. An description of the data sets used is then given, followed by the results and discussion chapter. Final remarks and suggestions for future research are then provided in the conclusion. Additional analyses of moisture distribution, flux, and net precipitation minus evaporation based upon alternate data sets are shown in the Appendix.

Chapter 2

METHOD

Three data sets from two sources were used in the moisture and latent heat transport calculations. Satellite based layer precipitable water content (PWC) measurements were used as the primary moisture data set. Analyses of relative humidity from the European Center for Medium Range Weather Forecasts (ECMWF) were used in separate transport calculations and converted to PWC fields for comparison with TOVS PWC fields (see the Appendix). The v-component wind analyses from ECMWF were used in all calculations of the poleward term of moisture flux.

2.1 PRECIPITABLE WATER CONTENT CALCULATIONS

Layer precipitable water content is defined as the vertical integral of the layer mean specific humidity,

$$PWC = \int_{p_1}^{p_2} \overline{q} \frac{dp}{g} \tag{2.1}$$

The original TOVS PWC fields were simply summed in the vertical to give total column value. Various time means of this daily data set are presented in the Appendix. No less than ten days of data were included in each TOVS monthly mean calculation. A missing data flag was assigned to that particular grid element if this threshold condition was not met.

ECMWF moisture data were available on a twice daily basis for all days of the study period, for all grid points, and at the standard pressure levels. These data were converted to layer mean specific humidity values as described in the data section. Only 1200 GMT analyses were used to reduce the volume of input data to one time per day. It is important

to note that the ECMWF analyses of relative humidity are for the specific time of 1200 GMT, while the daily TOVS sounding data is a composite of a large number of data collected throughout the 24 hour period centered on 1200 GMT. Analyses of ECMWF moisture distribution, and poleward transport are given in the Appendix.

2.2 ECMWF V-COMPONENT WINDS

Wind analyses from ECMWF remained largely unaltered from their original form to preserve the inherent quality of data therein. These fields were used at the original 2.5 degree resolution so no horizontal interpolation was necessary. In the vertical, however, winds at the standard pressure levels were averaged into layer means for use with the layer mean moisture data. As with the ECMWF relative humidity data, only 1200 GMT data were used.

2.3 POLEWARD LATENT HEAT TRANSPORT

In order to calculate poleward transport quantities, it is necessary to develop a set of mean statistics from which anomaly fields may be derived. Transport quantities were calculated based on monthly time means, a five year climatology, and time departures from these means. In addition, zonal averages were needed to derive the flow of latent heat across a given latitude, as described below.

Latent heat transport is just one of four components which make up the total atmospheric poleward heat transport. The total atmospheric energy flux (AT) into a polar cap described by latitude ϕ is the sum of the transport of sensible and latent heat, and potential and kinetic energy,

$$AT = \int_0^{p_0} \left[\left(C_p T + Lq + gz + \frac{1}{2}(v^2) \right) v \right] \left(\frac{2\pi a cos\phi}{g} \right) dp \tag{2.2}$$

This study deals only with that component which describes poleward latent heat transport (PLHT). In the zonal and monthly average,

$$PLHT = \int_0^{p_0} L\overline{[vq]} \left(\frac{2\pi a \, cos\phi}{g} \right) dp \tag{2.3}$$

where the overbar denotes a monthly average, and the square brackets represent a zonal average.

The highly averaged quantity, $\overline{[vq]}$, depends on three terms which have significantly independent physical meaning. The mean state of meridional transport is governed by the Hadley cell circulation where the near-surface branch carries very moist air toward the tropical belt of convergence where insolation is at a maximum. Further poleward, the stable subtropical high pressure cells move moist, primarily maritime air away from the subtropics toward midlatitudes. Finally, transient eddies in the midlatitude baroclinic zones transport available moisture into high latitudes. The three terms are defined as mean meridional circulation (MMC), transient eddy (TE) and standing eddy (SE) transport. The total transport is the sum of MMC, TE, and SE, respectively,

$$\overline{[vq]} = [\overline{v}][\overline{q}] + \overline{[v'q']} + [\,\overline{v^*}\,\overline{q^*}\,] \tag{2.4}$$

where, for a given variable A,

$[A]$ is the zonal average, $\frac{\pi}{2}\int A\,d\lambda$, λ is longitude,
$\overline{A}$ is the time mean, $\frac{1}{(t_2-t_1)}\int_{t_1}^{t_2} A\,dt$,
A' is the time departure from the climatological value, $A - \bar{A}$, and,
A^* is the zonal departure, A - [A].

Therefore, the poleward water vapor transport (PWVT) is,

$$PWVT = \int_0^{p_0} \left([\overline{v}][\overline{q}] + \overline{[v'q']} + [\,\overline{v^*}\,\overline{q^*}\,]\right)\left(\frac{2\pi a cos\phi}{g}\right) dp \tag{2.5}$$

where PLHT differs by the constant L, the Latent Heat of Condensation,

$$PLHT = L \cdot PWVT \tag{2.6}$$

The individual components were calculated independently and then summed for the total transport. A separate computation of the total transport is done by simply evaluating

the left hand side of Equation 2.4 directly. Comparison of the two methods gives a direct measure of the computational precision. An example is given in the Appendix.

In order to obtain the final transport data, it was first necessary to prepare certain statistics. Monthly and climatological means were calculated and then set aside for later use. The daily PWC and v-component wind data, as well as the above means, were used as input by the transport routine. Zonal and time departures could then be extracted and immediately used in the transport calculations. Vertical integration was done using the trapezoidal rule. Presented in the Appendix are analyses of ECMWF fields, and estimates of PLHT and precipitation minus evaporation by independent efforts.

2.4 EVALUATION OF PRECIPITATION MINUS EVAPORATION

Evaluation of the annual difference of precipitation minus evaporation, $\overline{[P-E]}$, is a logical extention of the annually averaged moisture transport. This quantity is derived by taking the derivative of the mean annual moisture transport in the absence of a storage term. Using a form of Eq. 85 from Lorenz (1967) for a general moisture balance equation in a latitude belt between ϕ_1 and ϕ_2,

$$\int_0^{p_0} 2\pi a\,(cos\phi_2 - cos\phi_1)\overline{[vq]}\frac{dp}{g} = -\int_0^{p_0}\int_{\phi_1}^{\phi_2} 2\pi a^2\, cos\phi \overline{\left[\frac{dq}{dt}\right]} d\phi \frac{dp}{g} \tag{2.7}$$

The net flux of moisture into an atmospheric column balances the difference in precipitation and evaporation rates (neglecting storage) as described in Lorenz (1967) Eq. 86,

$$\int_0^{p_0} \overline{\left[\frac{dq}{dt}\right]}\frac{dp}{g} = P - E \tag{2.8}$$

where P and E are precipitation and evaporation rates.

Using the above equations we can find the water balance equation for the annual mean as given by Lorenz (1967) Eq. 87, but from ϕ_1 to ϕ_2,

$$\int_0^{p_0} 2\pi a\,(cos\phi_2 - cos\phi_1)\overline{[vq]}\frac{dp}{g} = -\int_{\phi_1}^{\phi_2} 2\pi a^2\, cos\phi \overline{[P-E]}\, d\phi \tag{2.9}$$

Taking the derivative with respect to latitude,

$$\overline{[vq]}_{\phi_2} - \overline{[vq]}_{\phi_1} = -2\pi a^2 \overline{[P-E]} \int_{\phi_1}^{\phi_2} cos\phi \, d\phi \tag{2.10}$$

which gives the net annual precipitation minus evaporation rate between latitudes ϕ_1 and ϕ_2,

$$\overline{[P-E]} = -\frac{\overline{[vq]}_2 - \overline{[vq]}_1}{2\pi a^2 (sin\phi_2 - sin\phi_1)} \tag{2.11}$$

Annual zonal plots of $\overline{[P-E]}$ in 2.5 degree latitude belts using both ECMWF and ISCCP TOVS moisture data are given in the Appendix, as well as independent estimates of this quantity.

Chapter 3

DATA

Two distinctly different global data sets were used in determining poleward moisture transport over a study period of five years. Satellite based moisture retrievals were coupled with model analyses which use primarily land based information. Only minor adjustments were necessary to make the two data sets compatible in both time and space. Using the analyses from the two sources, fields of satellite precipitable water content, and model output v-component winds and precipitable water (as converted from relative humidity analyses) were utilized.

3.1 ISCCP TOVS PRECIPITABLE WATER MEASUREMENTS

Satellite based precipitable water measurements have been taken operationally since 1978 by the TIROS-N, or NOAA series of operational polar orbiting satellites (Schwalb, 1978). Utilizing a complement of seven orbiters, the NOAA system follows two previous operational programs. The Television and Infrared Observation Satellite (TIROS) research and development system, initiated on April 1, 1960, lead to the first operational U.S. polar orbiting satellite program, the TIROS Operational System (TOS) (for overview see Colorado State University, 1982). The launch of nine TOS Environmental Science Services Administration (ESSA) satellites were followed by six Improved TOS (ITOS) platforms which carried sensors capable of higher quality observations of the atmosphere. Since then, the NOAA series of satellites (TIROS-N, and NOAA 6-11) has provided uninterrupted global coverage by up to two satellites since the October 13, 1978 launch of TIROS-N.

The NOAA satellites have a near-polar sun synchronous orbit with a 102 minute period (Schwalb, 1978). The odd numbered orbiters (including TIROS-N) have afternoon ascending nodes, while NOAA 6, 8, and 10 have morning descending nodes. This orbital

conditions due to the opaque nature of clouds at these wavelengths. The TARM uses multispectral information to determine the number of cloudy FOV's, and if four or more are deemed clear, then the centroid of the clear FOV's describes the 250 km box based on the weighted average of the clear sky radiances. If fewer than four FOV's are clear, then the N*, or adjacent pair, method (Smith and Woolf, 1976) is used to extract a clear column radiance value from the partly cloudy scene. If the above methods fail, then the box is said to be cloudy, and radiances from channels not subject to cloud contamination are averaged to produce temperature soundings in the higher layers, where little water vapor is found.

The third module, the TIROS Stratospheric Mapper (TSM), applies limb corrections and maps SSU data to conform spatially to the HIRS/2 and MSU data. TSM output, along with output from TARM, is sent to the TIROS Retrieval Module (TRET). The TRET accesses a coefficient data base which is needed to generate the temperature and water vapor profiles as calculated by the method of eigenvector regression (Smith and Woolf, 1976). The weekly-updated regression coefficients are made using quasi-colocated radiosonde data, as well as space based radiance measurements, and are stratified within five latitude zones. Up to 25,000 soundings per day are theoretically possible using the above method, at the nominal 250 km resolution. However, a more modest figure of 8000 per day are operationally generated.

3.1.3 ISCCP and ISCCP TOVS

The operationally produced soundings are provided to the International Satellite Cloud Climatology Project (ISCCP) (Schiffer and Rossow, 1983) as an ancillary data set to the cloud data collected by geostationary and polar orbiting satellites (Schiffer and Rossow, 1985). An infrared radiation model uses the TOVS data to correct for water vapor absorption (Rossow, Garder, Lu, and Walker, 1988). The ISCCP version of the TOVS sounding product was used in the present study. To conform with the ISCCP cloud data format, the sounding data are fit to a 2.5 degree equal-angle grid, and interpolated to new layers in the vertical. This is done by subdividing the layer precipitable water content (PWC) into much smaller layers, assuming a constant relative humidity throughout the

original layers. The PWC for the small layers is summed within the new ISCCP defined layers, and adjustments to these new values are made to assure that no water was lost in the interpolation process. Small adjustments were made to the ISCCP TOVS moisture data so that it was fully compatible with the wind data set required for transport calculations. Vertical interpolation to slightly different levels was done by linear interpolation of specific humidity means. In addition, grid box values were converted to grid points.

The ISCCP data set, as used in the present study, consists of daily global fields for the five year period beginning in July 1983. As specified in Rossow and Kachmar (1988) a significant amount of data filling is required since daily observations only cover 66 percent of the grid. The daily fields are filled with monthly means, adjacent values, or climatological means, in areas of missing data. In addition, some grid points may be assigned a missing data flag due to observations outside a three standard deviation criterion. In all cases, an origin type value is assigned to each grid point. The present study uses only original TOVS data, and replaces all filled data with a separate missing data flag. This was done to prevent additional biases in the data which would show up in long term means, especially in regions of persistent cloud cover where either monthly means or climatological values would dominate. Nonetheless, areas of marine stratocumulus and tropical convection would still have data biases due to the inability of the TOVS package to retrieve soundings in such cloudy areas. Zonal and time means are biased toward drier, cloud-free conditions since missing data points are located, in many cases, in regions of relative moisture maxima. It is important to understand that moisture retrieval from space is done for bulk atmospheric layers, where a great deal of structure can be lost. Water vapor is a highly variable quantity in both time and space, and careful examination of existing data sets is key in deriving any useful information from them.

3.1.4 TOVS Evaluation

Early TOVS evaluation was done by Gruber and Watkins (1979) and showed the ability of the system to adequately sense atmospheric moisture content under certain conditions. In regions of cloud free air the retrieval scheme produces layer moisture values

strategy allows for a 90 degree orbital plane separation (to reduce the number of redundant observations) and thus up to four separate observations per day for a given region when two satellites are operational. A regular launch schedule was key in the continuous coverage by these satellites despite their relatively short two year expected lifetime.

3.1.1 The TIROS Operational Vertical Sounder

Carried aboard these platforms is the TIROS Operational Vertical Sounder (TOVS) instrument package for retrieval of atmospheric temperature, ozone, and water content. The TOVS system is made up of the second generation High Resolution Infrared Radiation Sounder (HIRS/2), the Microwave Sounding Unit (MSU), and the Stratospheric Sounding Unit (SSU) (Werbowetzki, 1981). The HIRS/2 and MSU are used for retrieval of vertical moisture profiles.

Both the HIRS/2 and the MSU instruments are cross-track scanners, capable of sensing a swath 2250 km wide. The HIRS/2 spectrometer has 19 infrared and one visible channel (see Fig. 3.1 for illustration of TOVS weighting functions), and are operated simultaneously during each scan. A HIRS/2 scan takes 6.4 seconds in 56 steps, with a field of view (FOV) ranging from 17.4 km at sub-satellite point, to a 58.5 km cross-track by 29.9 km along-track FOV at end of scan.

Calibration is performed every 256 seconds, or every 40 scans, to maintain accurate radiometric observation throughout the life of the sensor (Lauritson *et al.*, 1979). Operational calibration consists of using all channels to view an internal warm target, as well as space, to aid in converting Earth viewed radiometric counts to radiance values. The time equivalent of three scans is required for calibration, and no HIRS/2 data are collected during this time.

The MSU has four channels to sense radiation in the 5.5 mm oxygen absorption band. A MSU scan takes 25.6 seconds and consists of 11 steps, with nadir resolution of 109 km. Calibration is performed during nominal data collection which allows for uninterrupted MSU observation of the atmosphere. At the end of each scan, the spectrometer views space before observing two internal targets. These values are corrected with measurements

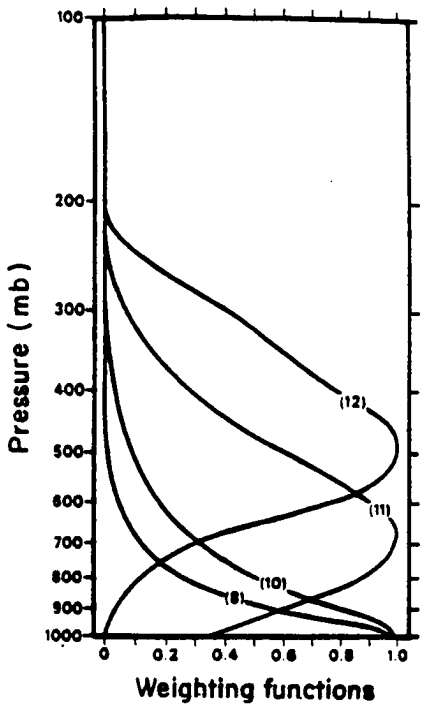

Figure 3.1: HIRS/2 weighting functions for the water vapor channels (10,11, and 12), and window channel (8) (after Werbowetzski, 1981).

made by platinum resistance thermometers and known National Bureau of Standards space radiometric values. The spectrometer then returns to start the next Earth-view scan.

3.1.2 TOVS Operational Retrieval Method

The individual scan spot data from the HIRS/2, MSU, and the third TOVS instrument, the Stratospheric Sounding Unit (SSU), is then processed to convert the 27 channel radiances to vertical profiles of temperature, water content, and ozone. The TOVS processing system consists of four modules (Werbowetzki, 1981), and is operated by the National Environmental Satellite, Data, and Information Service (NESDIS). Operationally ingested digital count data collected during one orbital period is fed into the TIROS preprocessor, which applies various corrections and calibrations, and appends navigational information to the output. The TIROS Atmospheric Radiance Module (TARM) takes the corrected single FOV radiance data from the preprocessor and produces soundings whose resolution is 250 km. The input single FOV data are grouped into 7 by 9 arrays for which tests for clouds are performed. Such tests are required since HIRS/2 infrared moisture channels, sensing radiation in water vapor absorption bands, can not be used under cloudy scene

comparable to quasi-colocated radiosonde observations. However, TOVS retrievals overestimate moisture content in high pressure regimes where dry, sinking air can be found. And since the retrieval scheme forces a profile that is representative of mean conditions, the dry scenario is not well represented. Similarly, deep moist layer water content is underestimated. Long term means of total column moisture are biased toward the land based mean conditions induced by the first guess fields generated from colocated radiosonde data. Anomaly fields have much less structure than would be expected due to the mean condition dominance. A recent evaluation of TOVS soundings, as compared with aircraft dropwindsonde data, over tropical oceans was done by Khalsa and Steiner (1987). While sharp features shown in the sonde data are not reproduced in the TOVS soundings, the bulk patterns are apparent. Nevertheless, stability indices calculated from the TOVS soundings are said to be useful.

Despite the obvious setbacks, use of this data set crosses a number of disciplines. TOVS soundings are operationally included in ECMWF analysis fields, and have a positive impact on the model produced forecasts (Illari, 1989). Research efforts include tropical atmosphere studies by Agarwal and Ashajayanthi (1983), and Steiner and Khalsa (1987).

3.2 ECMWF GLOBAL ANALYSES

In order to make moisture transport calculations it is important to secure a comprehensive global wind data set. Global analyses from the European Center for Medium Range Weather Forecasts (ECMWF) are of high quality and are widely accepted as the finest available. Dating back to 1979, the forecast model analysis fields have been archived in a consistent format for scientific research purposes. A product of the ECMWF forecast analysis and initialization scheme, the so called World Meteorological Organization (WMO) Archive contains the v-component wind data which is used, along with the ISCCP TOVS moisture data, to calculate poleward moisture transport. In addition, WMO Archive relative humidity data were used with the wind data for separate moisture transport calculations.

Primary goals of ECMWF focus on the use of high speed computers for numerical weather prediction. Data assimilation plays a key role in making accurate model predictions, and at ECMWF the initial state fields are generated in a multi-step process (Lönnberg and Shaw, 1986) which allows for the archival of these fields. The main elements of the assimilation scheme include data analysis, initialization, and forecast. Intermittent inclusion of new data and forecast information updates the fields before analysis and initialization. Initial state fields are then used in the global spectral forecast model for prediction in the medium range, and are archived for research purposes.

3.2.1 ECMWF Data Assimilation

Data are collected from a number of sources via the Global Telecommunications System (GTS). Nominal data types include surface, ship, buoy, and radiosonde data, pilot and aircraft reports, and satellite observations. Each data type undergoes a variety of quality control tests before use in the analysis (Lönnberg and Shaw, 1986). Data are compared with other observations from the same source, other adjacent observations, forecast values, and climatological data. The previous six-hour model forecast is used as the first guess field and is analyzed for error. Height and wind values are bound by the geostrophic relationship. Once interpolated to observation locations, the first guess field is subtracted from the observations and normalized by the first guess error. The three-dimensional analyzed fields are interpolated via the multivariate optimal interpolation scheme as presented by Lorenc (1981), taking into account the different error characteristics of each variable, and the error of the forecast. The analyzed fields are then subjected to nonlinear normal mode initialization (NNMI) to prevent amplification of anomalous high frequency gravity waves (see Williamson (1976) and Machenhauer (1977) for application of NNMI to the ECMWF initialization process). Moisture fields in the WMO Archive are fully analyzed and initialized, and more closely represent a so called "balanced" atmosphere than the original observations.

3.2.2 Use of the ECMWF Analyses

For use in the present study, the global ECMWF fields are used at the nominal resolution of 2.5 degrees, on an equal angle grid. In the vertical, level values are averaged into

layer means for compatibility with the layer mean satellite moisture data. The ECMWF winds are model output and therefore are reported at every grid point for each field. However, TOVS data is sparse, so the location of the satellite data defines which wind data points are used. Therefore, transport calculations involve only the grid points where valid TOVS data exist.

3.2.3 ECMWF Moisture Data

Poleward moisture transport was also calculated using ECMWF relative humidity data. Moisture data assimilation at ECMWF is handled somewhat differently than for other parameters. The ECMWF assimilation scheme accepts data from radiosondes, surface observations, and since 1985, satellite precipitable water estimates (Lönnberg and Shaw, 1986). Radiosonde dew point temperatures are converted to level relative humidity values, and assigned an error depending on the magnitude of the value. Surface reports are likewise used to generate a two meter relative humidity value. Cloud information within standard surface observations is used to estimate humidity in three tropospheric layers. Satellite precipitable water data from the TOVS package is interpolated to the five standard layers between the surface and 300 mb. Analysis is similar to that of mass and wind, except a univariate scheme is applied in layers below 300 mb. Inclusion of satellite moisture data in the analyses has little effect in the mean statistics (Illari, 1989). Therefore, comparisons of calculated transports using TOVS data vs. ECMWF moisture data are sufficiently different and are essentially independent.

Relative humidity fields are reported at five levels in the WMO Archive. The level data are converted to layer precipitable water content units by assuming a layer average relative humidity. Conversion to layer precipitable water requires knowledge of the layer mean specific humidity (q), which is derived using the mean temperature, saturation specific humidity, and relative humidity,

$$q = RH \cdot q_s \tag{3.1}$$

where,

$$q \approx \epsilon \frac{e}{p} \tag{3.2}$$

and,

$$\epsilon = \frac{R_d}{R_v} = 0.622 \tag{3.3}$$

Using the Clausius-Clapeyron relation with known T it is possible to obtain the saturation vapor pressure,

$$e_s = e_{so} exp\left[\frac{L}{R_v}\left(\frac{1}{T_0} - \frac{1}{T}\right)\right] \tag{3.4}$$

where L is the latent heat of condensation, and T_0 is the reference temperature of 273.15 K.

The saturation vapor pressure, along with the mean pressure, gives the saturation specific humidity as per above. The layer mean saturation specific humidity is used along with the mean relative humidity to give the mean specific humidity. Therefore, using these derived values, the precipitable water content (PWC),

$$PWC = \int_{p_1}^{p_2} \bar{q} \frac{dp}{g} \tag{3.5}$$

was used to generate global ECMWF moisture fields as shown in the Appendix.

3.2.4 Evaluation of ECMWF Global Analyses

An evaluation of ECMWF analyses over a seven year period is given by Trenberth and Olson (1988). Changes in the the ECMWF analysis scheme and model code have resulted in periodic adjustments to the analysis fields. Time series of areally averaged quantities such as geopotential height, wind, and humidity are shown to have a fairly stable nature over the study period, with some exceptions. Examination of the 700 mb average humidity between 20N and 20S reveals a large adjustment on May 1, 1985. This was due to changes in the physical parameterization scheme and the new representation of clouds in the model. Other smaller adjustments related to model changes are seen in the time series and are documented by Pasch and Illari (1985), and Trenberth and Olson

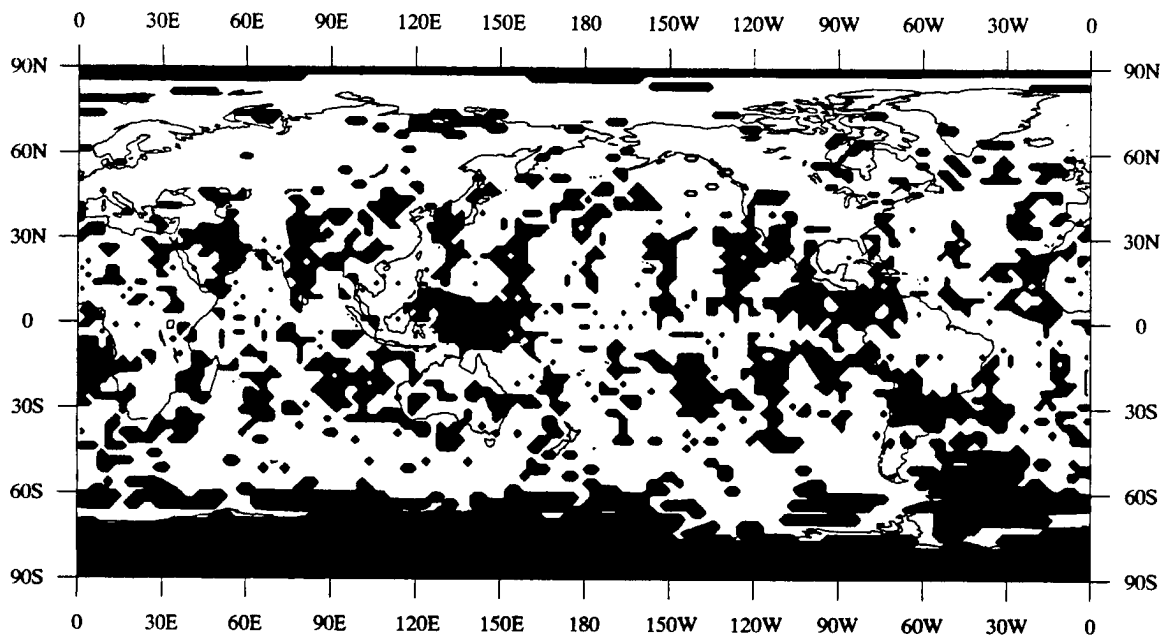

Figure 4.1: An example of data coverage for a daily composite of TOVS moisture retrievals. Shown here is the July 1, 1983 field. Shaded areas represent missing data.

available data sets could be used in a comparison. The additional data are presented in the Appendix.) In a broad sense, this monthly mean field has properly represented features, such as a maximum PWC area along the Intertropical Convergence Zone (ITCZ), minima over high latitude land areas and elevated terrain, and gradients near continental margins. The high values in the tropical eastern Pacific encompass a large area, and extend westward into the Indian Ocean. Large evaporation rates from warm ocean surfaces here provide the source for large atmospheric PWC values. An additional maximum is found in the western Pacific where an active ITCZ over a similarly warm ocean surface produces numerous tropical disturbances each summer and fall. High values are seen here even though persistent cloud cover allows for a reduced number of retrievable observations per month for many grid areas. The minimum number of observations per month (10) is generally exceeded in this region, however.

All large elevated land masses, such as the Andes, the western U.S. Plateau, and the Tibetan Plateau, lie beneath minima in PWC in the September 1987 monthly mean. Lower land areas, such as the eastern U.S., Brazil, Siberia, and Australia, all exhibit lower values than oceans at similar latitudes. The absolute minima occurs over Antarctica where a cold, dry winter is ending. Orbital constraints prevent the NOAA satellites from obtaining data at the highest latitudes, so data here is largely missing. Climatological values would be suitable for use here since absolute values are very low. However, a high percentage error may occur for this very reason. The present study used no such data, and therefore a large percentage of data poleward of 70 degrees is missing. Contributions from high latitude PWC toward a hemispheric or global average using only clear air data are somewhat biased toward a slightly higher value. The absolute magnitude of this bias is presumed to be small due to the small area at such high latitudes.

An annual mean field example is shown in Fig. 4.3 which exhibits features that are more smoothed in nature as compared to the monthly mean example. The annual average example shows a well defined ITCZ, as well as a South Pacific Convergence Zone (SPCZ) which is oriented along an axis running from just southeast of the Phillipines toward the east-southeast. The ITCZ annual mean latitude lies in the Northern Hemisphere, at five

(1988). Irregardless of periodic changes, the analyses were deemed useful in providing an alternative source of PWC and transport calculations.

Changes to the analysis and forecast schemes at ECMWF are done to improve model output quality, and less emphasis is placed on generating analysis fields that are climatologically consistent in nature. Therefore, adjustments in the output statistics have significant impact on the analysis climate. It was deemed beyond the scope of this thesis to remove all discontinuities from the analysis fields. While the ECMWF moisture data are highly sensitive to changes in the model and analysis code, they are used here simply to provide for an independent calculation of moisture transport.

Chapter 4

RESULTS AND DISCUSSION

The characterization of large scale moisture distribution and transport requires careful examination of the available global data sets. In the present study, satellite based precipitable water content (PWC) analyses are examined on time scales as short as one day, and as long as a five year period. Together they provide for an adequate characterization of the global moisture distribution. It is therefore possible to examine the physical information provided while being aware of factors which influence the quality and representativeness of the data. Similarly, poleward transport calculations using the daily wind and moisture information are analyzed, and complement earlier ground based estimates. In addition, new information over the data sparse Southern Hemisphere are given.

4.1 PRECIPITABLE WATER CONTENT MEASUREMENTS

Daily data is composited using measurements from either one or two operating polar orbiting NOAA satellites. Data coverage is somewhat less than total, and adjacent measurements may have been taken up to 24 hours apart. Therefore, the daily fields are not consistent in time and space. An example of a daily field is shown in Fig. 4.1. The typical daily field has approximately two thirds of total areal data coverage while the remaining area of missing data is due to gaps in the individual scans, between scans, and where data retrieval is not possible in cloudy scenes. Daily data can be used in smaller scale applications, but are presently used in time averages on a global scale to understand the longer term global distribution of PWC.

When used in a monthly mean, the data shows recognizable patterns and no longer suffers from significant data loss. Fig. 4.2 shows the global distribution of PWC for the month of September, 1987. (This particular month was chosen so that two other

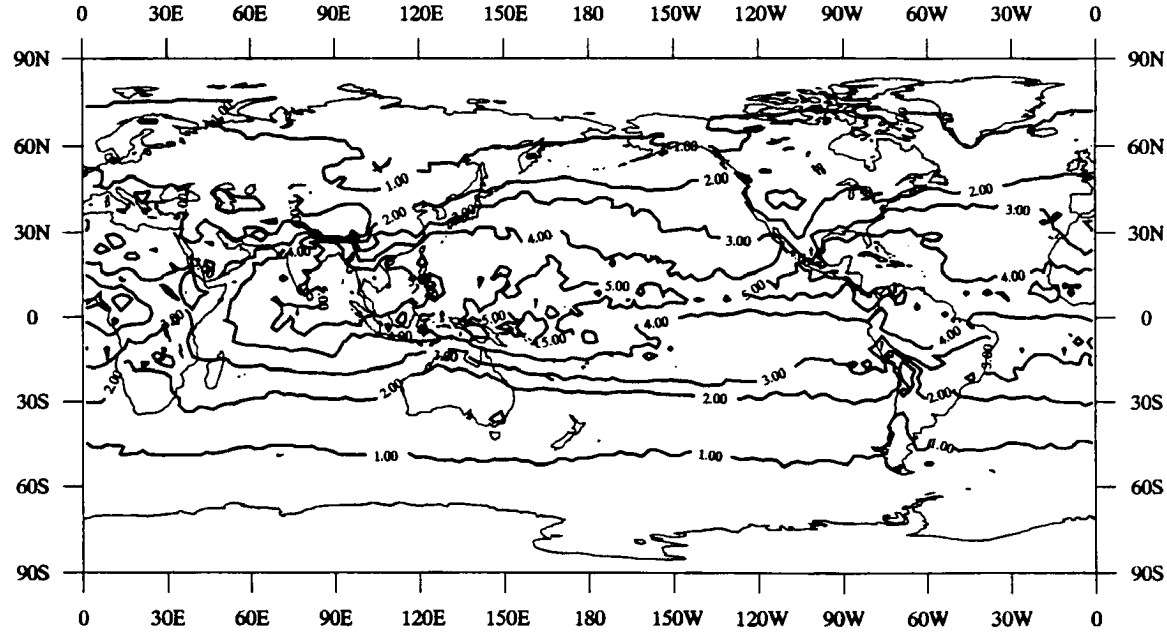

Figure 4.2: Monthly average of ISCCP TOVS precipitable water content for September, 1987.

degrees north of the equator. Mean meridional circulation within the strong NH Hadley cell, as well as the land locked subtropical high pressure cells, are responsible for the net annual northward deviation from the equator of the ITCZ. Weaker and less persistent subtropical highs in the SH have less impact upon the mean position of this convergence zone as the NH circulations are more persistent throughout the year. Cross-equatorial flow of moisture (as well as other quantities such as heat and energy) is therefore implied in the annual mean. This has important consequences for certain large scale atmospheric phenomenon, such as the Indian monsoon circulation and related precipitation potential, and the formation of tropical cyclones in more favored regions further away from the equator.

The five year mean climatology, as shown in Fig. 4.4, shows a similar data field, only further smoothed. All features are slightly different from the 1987-88 annual mean case, showing that there is some variability from year-to-year. In all mean field cases, from monthly to climatological, the mean state of the atmosphere is relatively well represented. However, long term averages of high frequency variations within the moisture field tend to be absent. The TOVS retrieval scheme forces values toward latitudinally stratified averages based on land based radiosonde data, which introduces a bias toward a mean, cloud-free state. A time mean of one month duration should yield some sign of persistent cross-latitudinal flow, where poleward moisture transport is located along the periphery of a stationary high pressure area. The September 1987 mean TOVS data shows no sign of this while microwave measurements made during this month showed a pronounced north-south moisture axis in the eastern Pacific from 30 to 50 degrees north (see the Appendix for September 1987 Special Sensor Microwave / Imager (SSM/I) data).

The effect of data omission in the TOVS fields has somewhat important implications. Since a significant amount of moisture is moved poleward in mesoscale to synoptic scale systems which have predominant cloud cover, a negative bias is introduced in these areas where moisture values are significantly greater than the zonal average. Phenomena such as "moisture bursts", as studied by McGuirk (1987), are now known to play an important role in transporting moisture out of the tropics. These and other relatively narrow streams

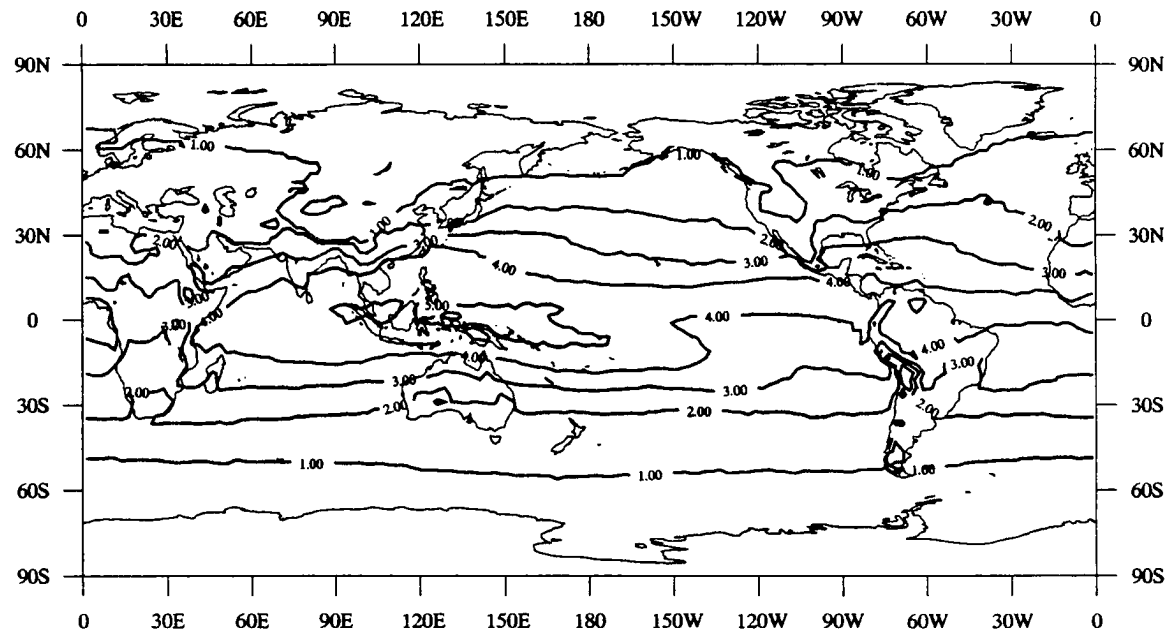

Figure 4.3: Annual average of ISCCP TOVS precipitable water content for the year beginning on July 1, 1987.

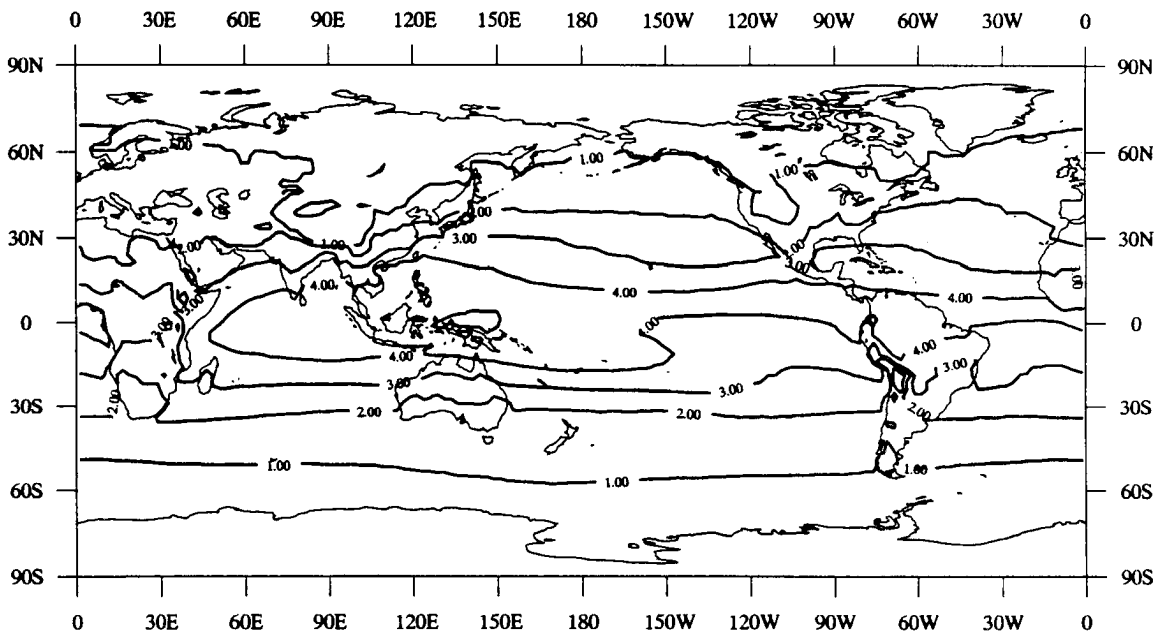

Figure 4.4: Mean ISCCP TOVS precipitable water content for the five year period of July 1, 1983 through June 30, 1988.

Table 4.1

Various estimates of hemispheric and globally averaged precipitable water content in centimeters.

Investigator	Data	Time Period	NH	SH	GL
Present study	TOVS	1983-88	2.43	2.26	2.35
Present study	ECMWF	1983-88	2.87	2.61	2.74
Rosen *et al.*(1979)	MIT	1958-63,68	2.57		
Trenberth (1981)	sfc based	many			2.53
Trenberth (1987)	ECMWF	1978-85			2.86

of moisture must be adequately characterized to fully understand the contribution of moist transient systems to the global mean state of the moist atmosphere. Long term averages of data sets not sensitive to high frequency variations of moisture will be biased toward a lower background, or undisturbed state.

Estimates of annual hemispheric and globally averaged PWC are given in Table 4.1. Three independent estimates are added and are primarily based on analyses of radiosonde measurements and have relatively little ocean data coverage. An average of the TOVS moisture and the analyzed ECMWF moisture content compare very favorably with the estimate by Rosen *et al.* (1979). The ECMWF moisture is generally reported to be an overestimate, while the TOVS data tends to underestimate the actual conditions due the lack of any contribution in cloudy areas, which are regions of relative maxima. The true value for the Northern Hemisphere (NH) PWC average is likely to be very near the aforementioned independent estimate. Similarly, the mean of the globally averaged ECMWF and TOVS data sets corresponds very well with the global average reported by Trenberth (1981). His estimate of the surface pressure contribution of global water vapor may be the most accurate to date. Therefore, a relatively high level of confidence may be placed on this particular quantity.

It is interesting to note the large difference in northern versus Southern Hemisphere values for the annual mean. NH values are substantially larger than those of the Southern Hemisphere (SH) due to the asymmetry of land mass distribution between the two. The elevated NH values are due to increased lifting of air over land, providing for a much

deeper mean moisture profile. Fig. 4.5 shows a time series of five annual cycles of NH, SH, and global (GL) monthly averages. The larger NH annual cycle is apparent, with much higher warm season values that peak most frequently in August. Minima for both hemispheres have similar magnitude, showing the similarity of mean moisture in the more stably stratified cold season atmosphere. The slightly less moist NH minima show the effects of cold and dry interior land areas.

The TOVS data set is presumed to have fairly consistent data quality for the time period chosen. Biases over time due to changes in the retrieval scheme are not significant enough to show up in annual mean, and therefore year-to-year fluctuations in an area average are presumed to be real. Interannual variations of zonally averaged PWC are shown in Fig. 4.6. Peak PWC values near 10N vary as much as 0.2 cm from the driest year to the wettest. However, the zonal PWC profile maintains a very similar shape for all five yearly means. Variability from one year to the next at a particular latitude is small, but some noticable change is evident. The last two years of data revealed higher tropical mean PWC values while midlatitude values were lower than the previous years. Likewise, the 1983-84 mean was smallest in most of the SH and in the NH subtropics, but was largest of all years in the NH midlatitudes above 45N. Therefore, for a given year, positive anomalies at one latitude are complemented by negative anomalies at a somewhat different latitude. For the most part the anomalies are balanced, and interannual hemispheric variations are much smaller than seasonal fluctuations within a given annual cycle. Table 4.2 shows the five year averaged seasonal hemispheric and global means. Large seasonal fluctuations exist in the NH where land has an important influence on atmospheric moisture content and distribution.

4.2 POLEWARD LATENT HEAT CALCULATIONS

Coupled with the ECMWF analyzed v-component winds, the TOVS moisture data is set into motion as a transport quantity. Broken down into three independent contributing components, the total poleward water vapor transport (PWVT) may be carefully analyzed. Total poleward latent heat transport (PLHT) is also obtainable, as this quantity is

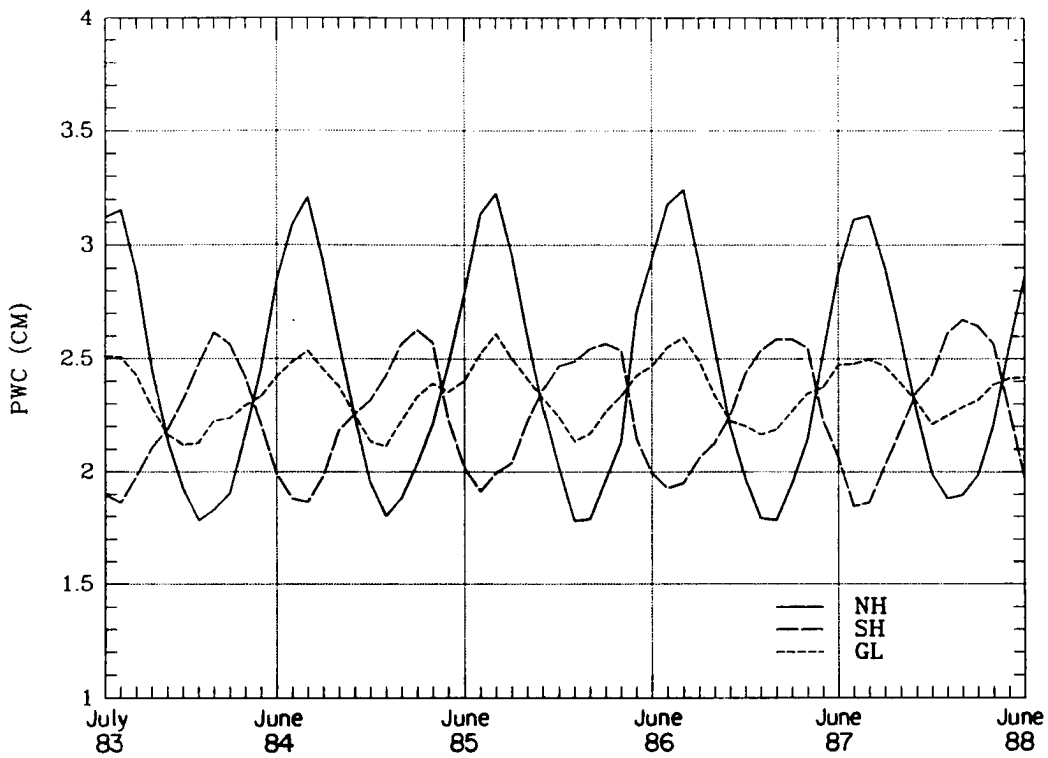

Figure 4.5: Time series of hemispheric and globally averaged ISCCP TOVS precipitable water content during the five year study period.

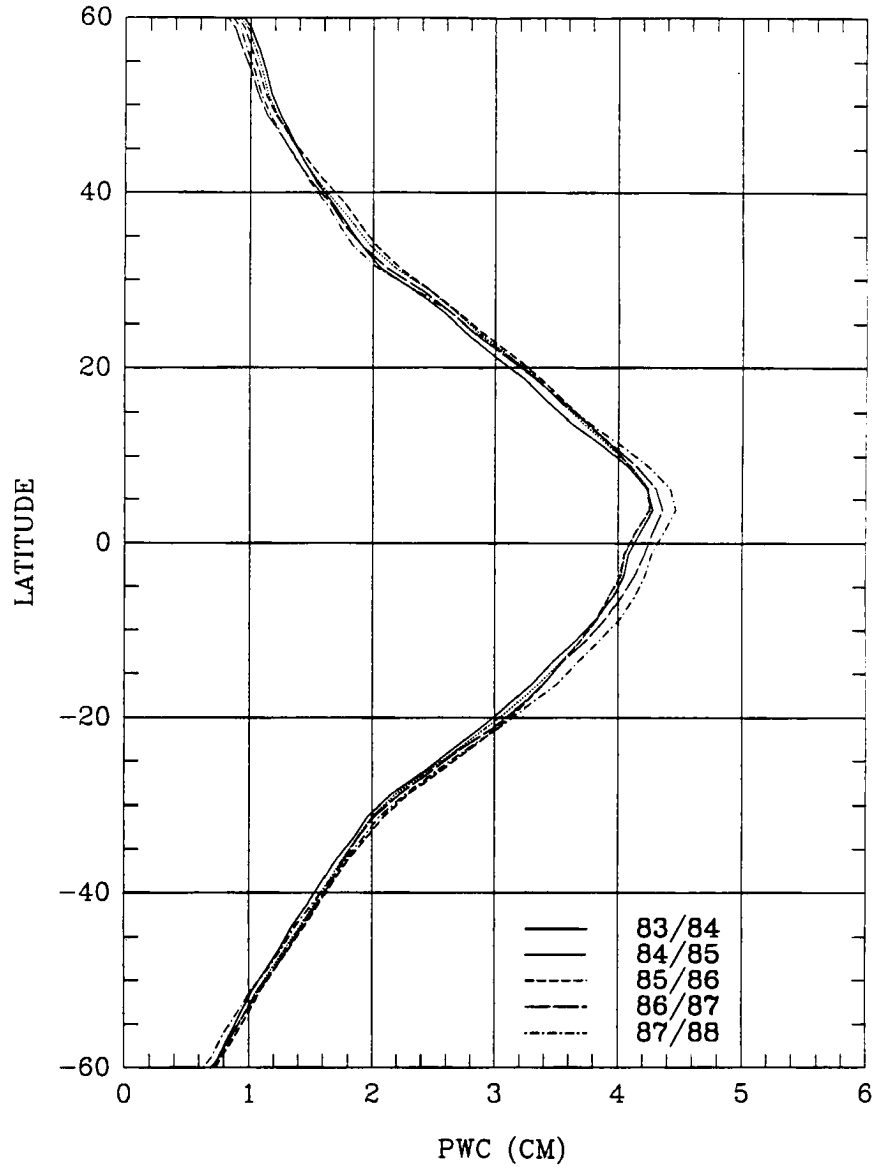

Figure 4.6: Annual zonal averages of ISCCP TOVS analyzed precipitable water content. Each annual average represents July through the following June.

Table 4.2

Average seasonal hemispheric and globally averaged PWC (in centimeters) based on five years of data. JJA is the northern summer defined by June, July, and August.

Season	NH	SH	GL
JJA	3.08	1.94	2.51
SON	2.25	2.28	2.27
DJF	1.87	2.57	2.22
MAM	2.53	2.25	2.39

different by only a constant. Analyses of total PLHT are given so that an estimate of the contribution to the total poleward heat transport may be derived.

The three independent transport components each play an important role in moving latent energy from one latitude to the next. The low latitude circulation is dominated by the thermally direct Hadley cells, which move warm, moist, low level air toward the ITCZ. In general, this trade wind flow encounters its counterpart from the opposite hemisphere along the ITCZ. This tropical circulation dominates the total transport in any given month. Eddy transport in higher latitudes carry latent energy toward the poles. Subtropical high pressures cells, which are more apparent in the NH, provide a persistent vehicle for transport. Finally, midlatitude cyclonic systems complement the standing eddies by moving large amounts of latent energy poleward in smaller spatial extents. An example of PLHT for a particular month is given in Fig. 4.7. The three components, as well as their sum, are shown. The dominance of the mean meridional circulation (MMC) at low latitudes is readily apparent. During the month of September 1987, over 4.5×10^{15} watts, or 4.5 petawatts (PW) of northward latent energy is moving through the tropics near 5S. Moisture (and therefore latent energy) converges near 15N as southward NH transport meets the opposite incoming low level flux from the SH. Hemispheric transient eddy (TE) contributions peak at near 50N and 40S, while stationary eddy flux peaks can be found at just poleward of 20 degrees in both hemispheres. The three components are additive in the midlatitudes, where a mix of both mean flow, and eddies are found.

The magnitude of the MMC is likely to be fairly accurate, while eddy terms are not well represented. The persistent MMC, containing high PWC values and modestly strong

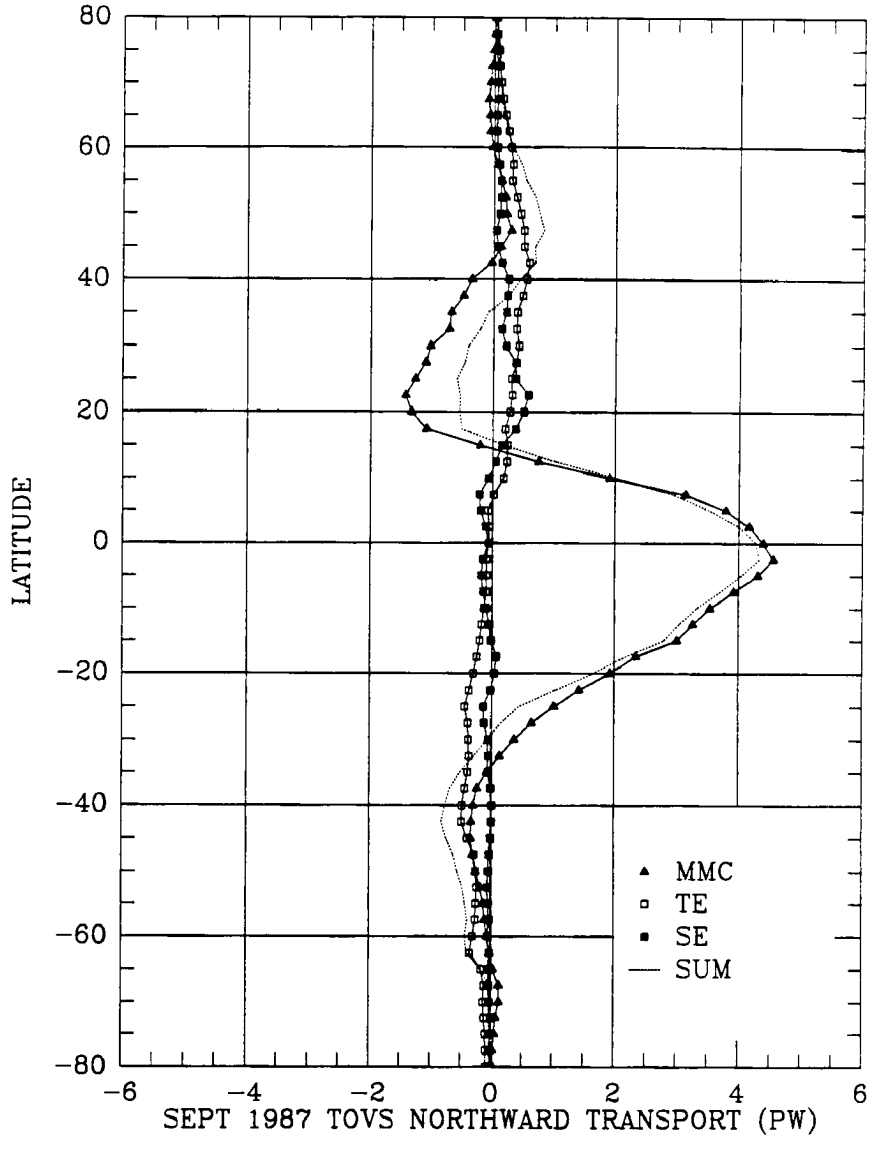

Figure 4.7: September, 1987 northward latent heat transport of the mean meridional circulation (MMC), transport by transient eddies (TE), standing eddies (SE), and the total transport (SUM) based on ISCCP TOVS moisture and ECMWF wind fields.

low level winds, is not likely to be underestimated by much, if any. A few observations in low latitudes are more likely to better represent the monthly mean there than similarly at higher latitudes. Midlatitude eddies are largely ignored by the TOVS retrieval scheme since a majority of these features are associated with predominant cloud cover, and therefore rendering the infrared moisture-sensing instruments useless. (Data from the ECMWF relative humidity analyses were used to generate similar transport curves, and the September 1987 case is shown in the Appendix.)

Midlatitude PWVT has been shown to peak during the months of April and November (Oort, 1971). Using data from the five April months within the study period, a climatological April field (Fig. 4.8) is obtained. Fig. 4.9 shows the averaged November case. In both months, all terms are fairly symmetric about the equator, and both the MMC and total transports (labeled SUM) change sign precisely there. The November MMC shows some asymmetry at low latitudes due to the influence of land areas. Transient eddy values are very similar in both months, as these are the transition periods from the cold season to the warm season, and vice versa. Slightly higher November TOVS SH values exist where the dominance of eddy circulations is more pronounced during the active spring season. Transport by the stationary eddies is also quite symmetric about the equator. Peak values in the NH are larger than those in the SH, and the relative magnitude of the SE transport is smallest of all three components at many latitudes. Southern Hemisphere SE transport never exceeds an absolute value of 0.3 PW. Northern Hemisphere transient eddy transport is at a maximum during April and October, while peak SE values have maxima in July for the NH, and January for the SH, as shown in Figures 4.10 and 4.11 (values of each component are plotted at latitudes where the highest zonal averages are found). Peak TE transport in October occurs a month earlier than was previously reported by Oort (1971). A multi-year data set was also used, so it is presumed that months of peak transport should coincide. Presumably, more midlatitude cloud cover one month later obscures the peak signal for November. The TOVS data shows an April TE maximum, however, which is consistent with the Oort study. The SE transports have a pronounced annual cycle, and are of greater magnitude in the NH. While the magnitude of the eddy transports in the

SH is likely to be too small, the asymmetry of both TE and SE transport is assumed to be real (see Figures 4.10 and 4.11). As would be expected, transport by transient eddies have similar magnitudes in both hemispheres, and NH stationary eddy transport is larger than in the SH during each climatologically represented month.

In the annual mean, a number of new features emerge in all components of the PLHT. Three of five sets of annual means are shown in Figures 4.12,4.13, and 4.14. As in the previous figures, some patterns are fairly well represented, while other features are inconsistent with both earlier independent estimates and other time periods within the present data set. For example, the magnitude of the total transport within the tropics and subtropics grows significantly from the 1983-84 case to much larger values in 1987-88. Obviously due to increased annual MMC transport, the total transport shows the effects of changes in the ECMWF model (Trenberth and Olson, 1988). Specifically, in 1985, the spectral resolution increased and parameterizations of convection, clouds, and large scale condensation. Further changes were made in 1986 which are responsible for the additional amplitude seen in the 1987-88 case.

Changes in the ECMWF model winds far outweigh changes in the TOVS moisture retrieval method, so much of the interannual variability seen in the annual transports is spurious. However, some real information does exist and can be extracted while being aware of the effects of these changes. Midlatitude transports are additive in the annual mean, and act to move latent energy poleward throughout the year. Peak values lie between 40 and 50 degrees latitude in both hemispheres as shown in Figures 4.12, 4.13, and 4.14. All components peak at different latitudes which shows that the three processes act to move moisture poleward (or equatorward), and are predominantly independent of the others at most latitudes. In general, TE transport is the most symmetrical about the equator, while SE peak values are higher in the NH. The MMC undergoes significant change with time, as discussed above, and exceeds the magnitude of midlatitude transport in all but the 1983-84 case. Here the annual tropical values are less than those during any given month, so some cancellation is seen due to the variation within the annual cycle. Typical monthly peak MMC values are greater than 3 PW, while the 1983-84 annual

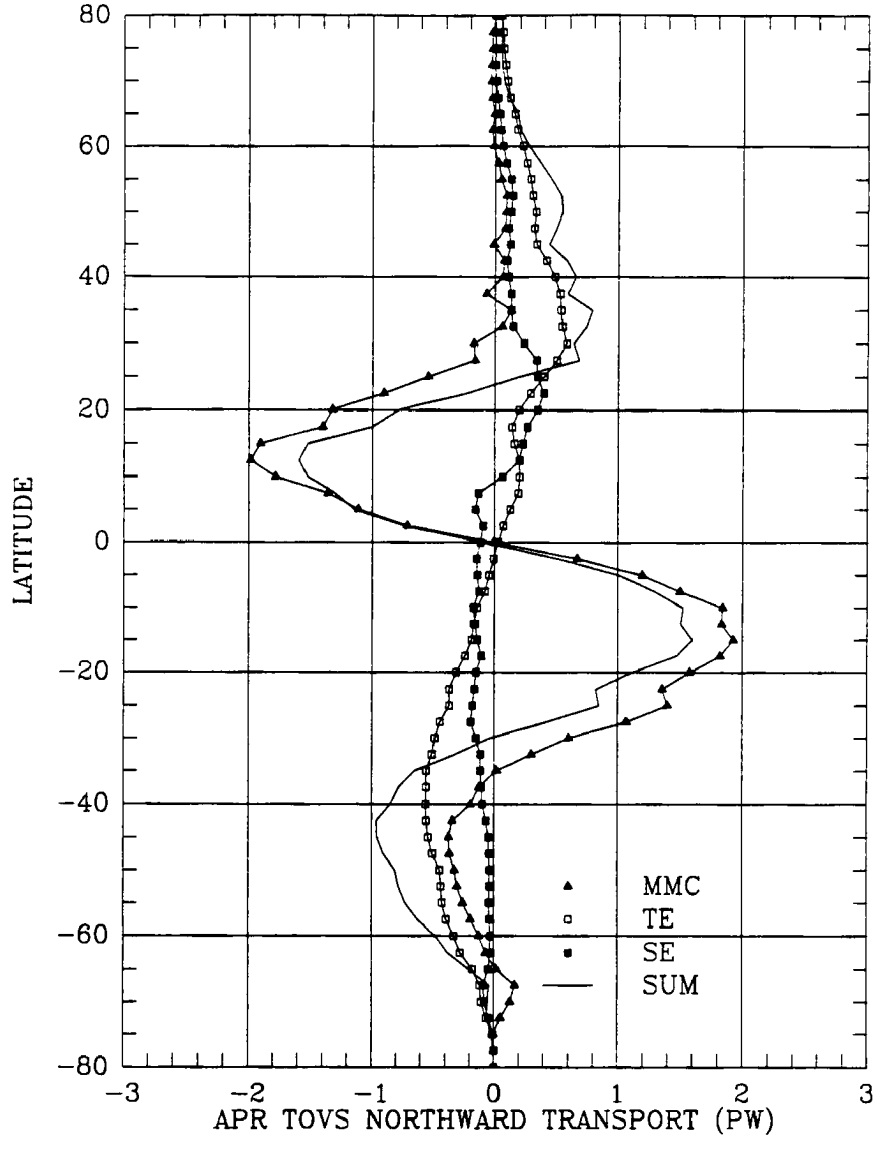

Figure 4.8: Northward latent heat transport of the mean meridional circulation (MMC), transport by transient eddies (TE), standing eddies (SE), and the total transport (SUM) based on ISCCP TOVS moisture and ECMWF wind fields for the average of five April months from 1984 to 1988. The computed total transport is labeled VQ. Units are petawatts.

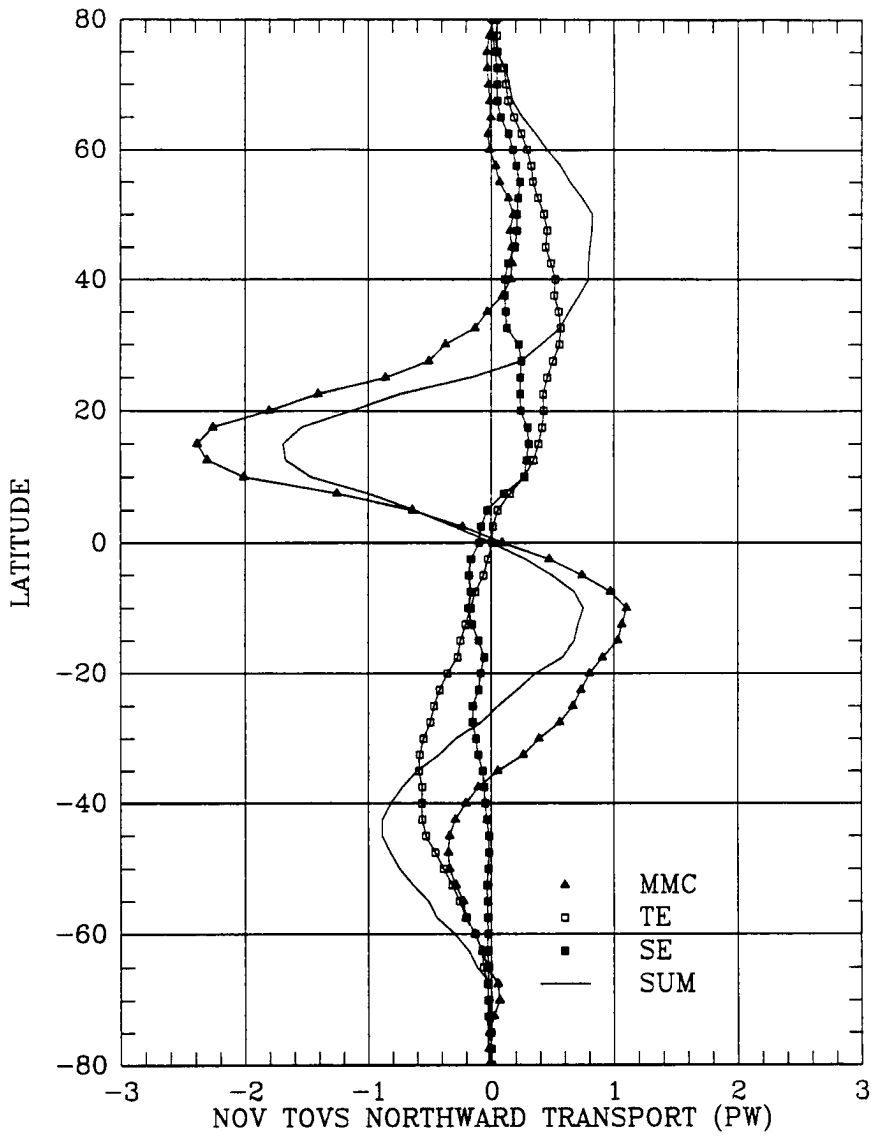

Figure 4.9: Northward latent heat transport of the mean meridional circulation (MMC), transport by transient eddies (TE), standing eddies (SE), and the total transport (SUM) based on ISCCP TOVS moisture and ECMWF wind fields for the average of five November months from 1983 to 1987. The computed total transport is labeled VQ. Units are petawatts.

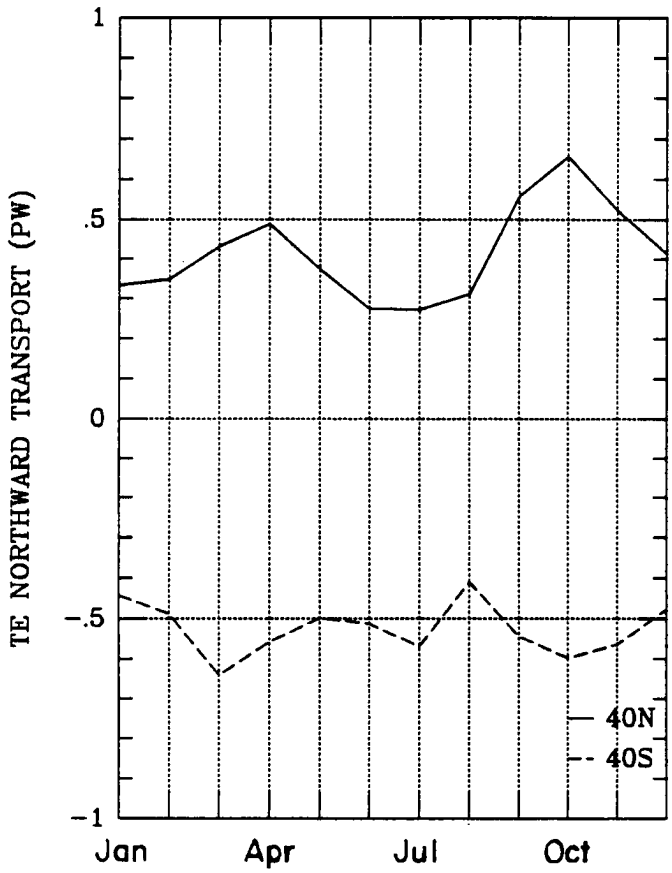

Figure 4.10: Annual cycle of latitudinal peak transient eddy latent heat transport based on ISCCP TOVS moisture and ECMWF wind data. Units are petawatts.

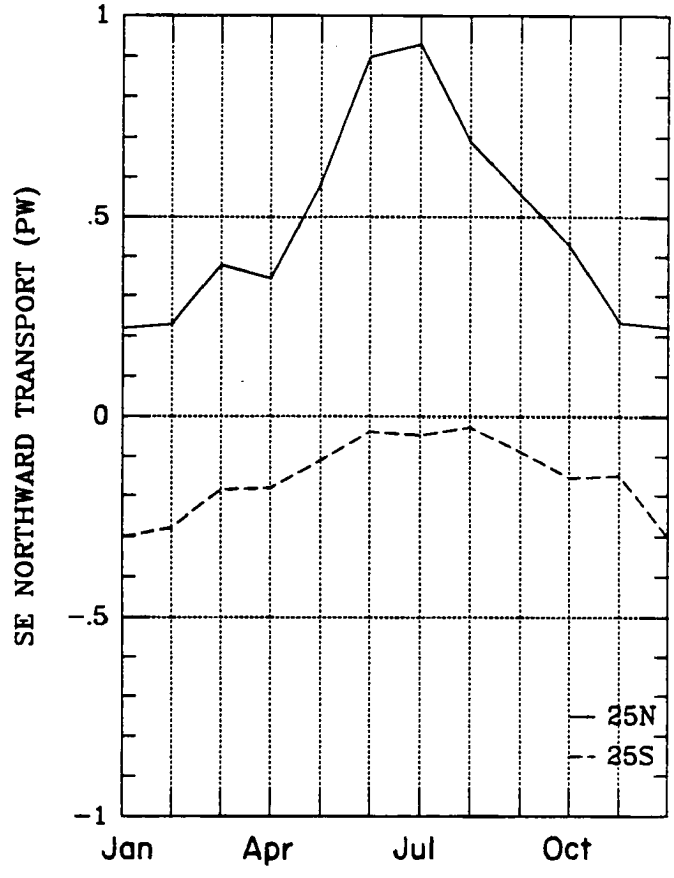

Figure 4.11: Annual cycle of latitudinal peak standing eddy latent heat transport based on ISCCP TOVS moisture and ECMWF wind data. Units are petawatts.

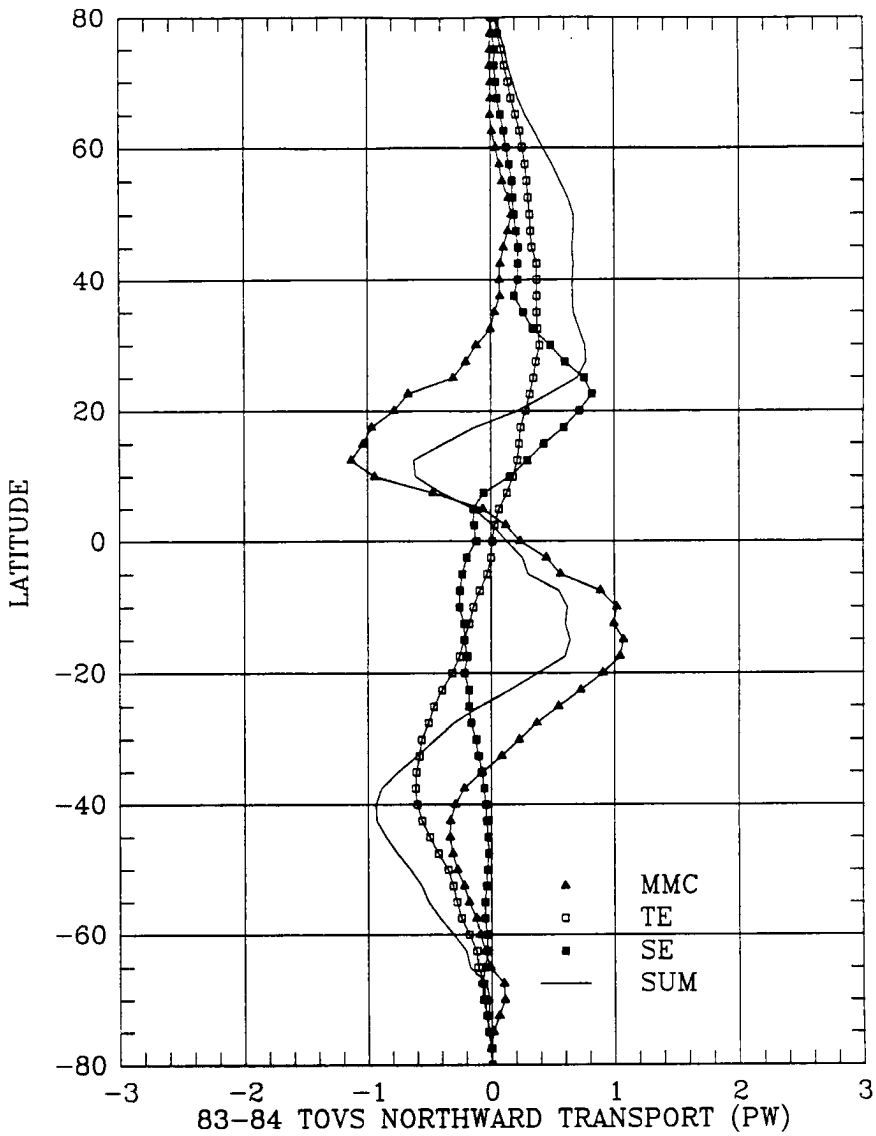

Figure 4.12: Annual average of the northward latent heat transport of the mean meridional circulation (MMC), transport by transient eddies (TE), standing eddies (SE), and the total transport (SUM) based on ISCCP TOVS moisture and ECMWF wind fields for the year beginning on July 1, 1983. Units are petawatts.

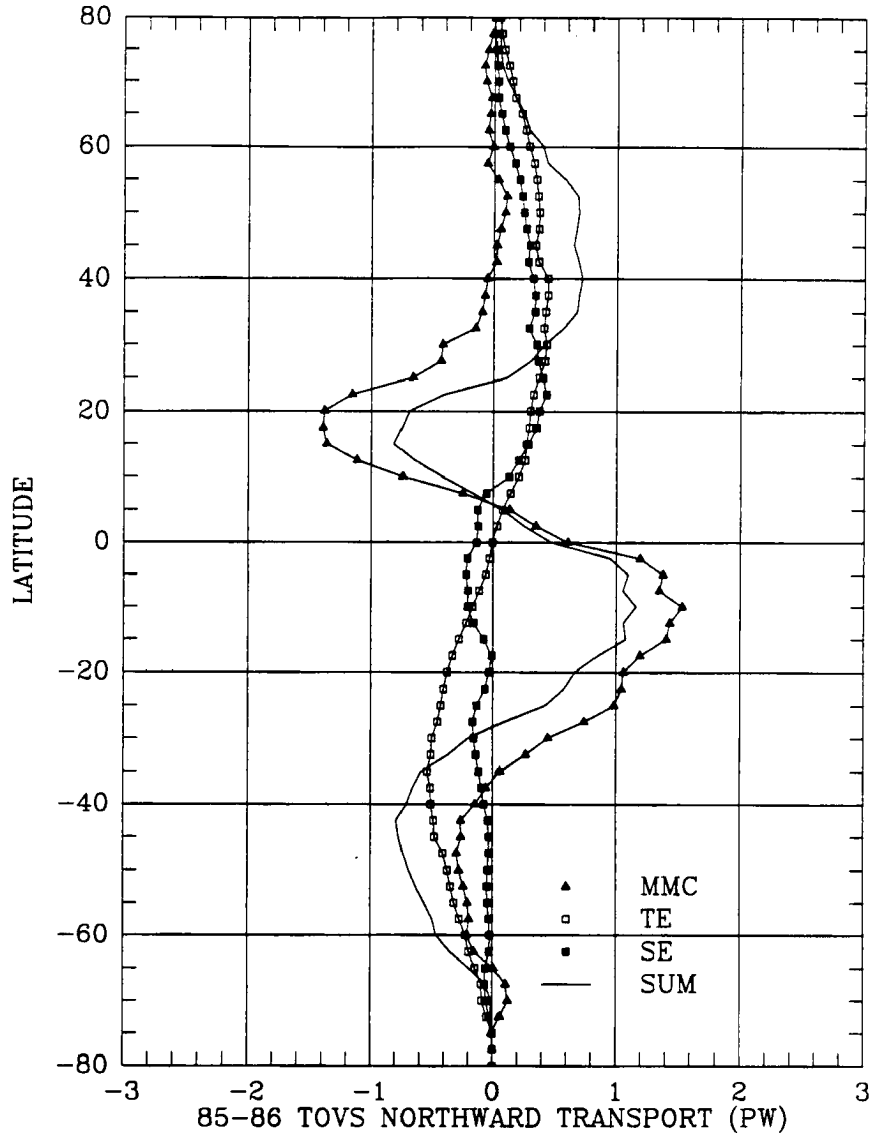

Figure 4.13: Annual average of the northward latent heat transport of the mean meridional circulation (MMC), transport by transient eddies (TE), standing eddies (SE), and the total transport (SUM) based on ISCCP TOVS moisture and ECMWF wind fields for the year beginning on July 1, 1985. Units are petawatts.

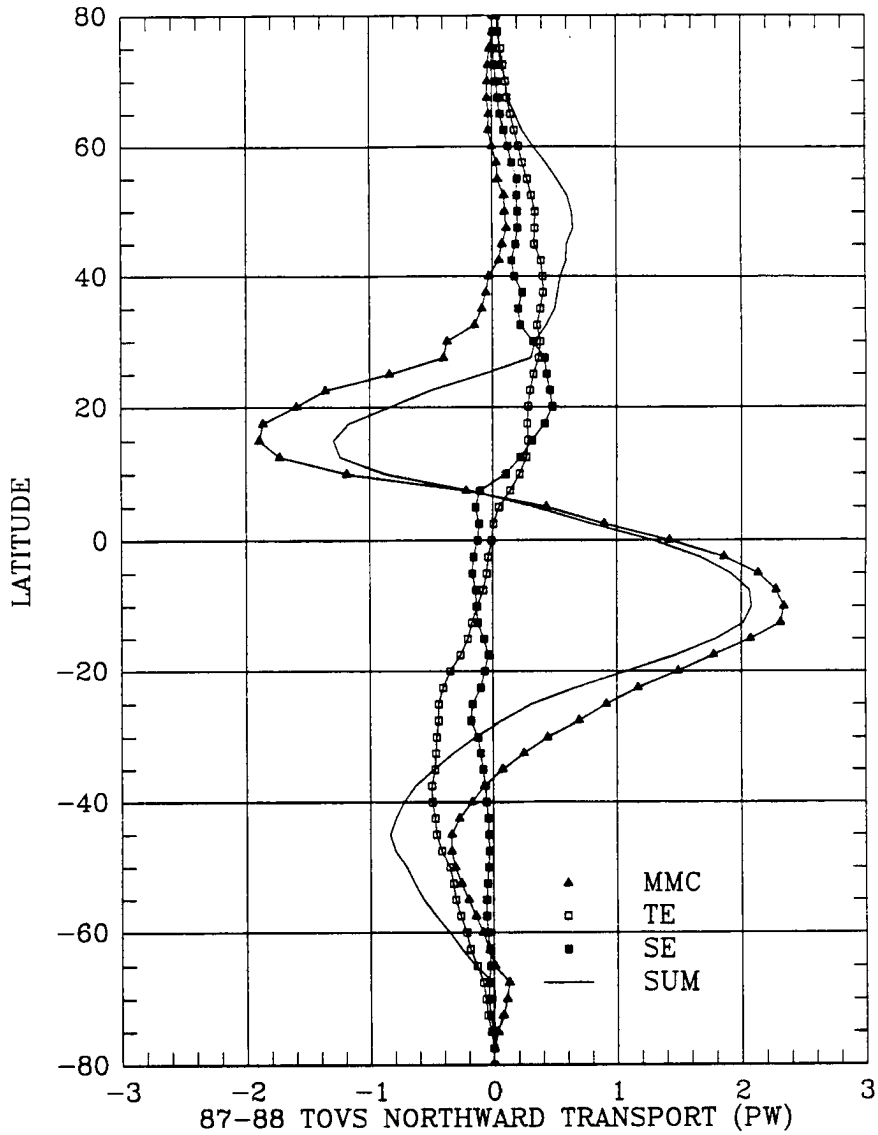

Figure 4.14: Annual average of the northward latent heat transport of the mean meridional circulation (MMC), transport by transient eddies (TE), standing eddies (SE), and the total transport (SUM) based on ISCCP TOVS moisture and ECMWF wind fields for the year beginning on July 1, 1987. Units are petawatts.

mean shows peaks of approximately 1 PW. While changes within the ECMWF model are assumed constructive, it appears that the best represented transports using such data are for the first year studied, or 1983-84. Previous estimates by Oort (1971) show this sort of pattern, where tropical transport tends to cancel in the annual mean, and midlatitude poleward moisture flux is additive. The magnitude of the following annual tropical MMC transports increases to unbelievable levels, and therefore is not accepted (see Figures 4.13 and 4.14). However, MMC and SUM transport values change sign at 5 degrees north, precisely where the mean ITCZ position is found. This result highlights the ability of the present data sets to accurately locate regions of large gradients in the total tropical transport. Positions of peak fluxes in midlatitudes are less likely shown at correct latitudes due to the aforementioned cloud cover problem.

While patterns within the midlatitude change from year-to-year, they are more believable than those in the tropics. Since the TOVS data set is relatively consistent with time, and the ECMWF spectral model was originally designed to best handle midlatitude meteorology, transports calculated using the two data sets are most temporally consistent there. Only the magnitude is likely to be in error, due to the inability of the TOVS infrared sensors to see through clouds. Fig. 4.15 shows the five zonally averaged annual total PLHT curves. Two dominant features are dramatically shown. Interannual consistency of the midlatitude values is contrasted by the widely varying tropical values. The latitude where northward transport switches sign in the tropics (at the mean ITCZ position) varies widely from 2.5N to 10N. Tropical values at 10N and 10S are generally higher during the last three years of the study. Unfortunately, much of the variability within the tropics is due to ECMWF model changes that affected the wind fields. Independent estimates of the interannual profiles are given in the Appendix to provide additional information for comparison.

4.3 ESTIMATES OF NET ANNUAL PRECIPITATION MINUS EVAPORATION

As described in the method section, annual moisture transport values may be differentiated in latitude to give annual net precipitation minus evaporation, when storage is

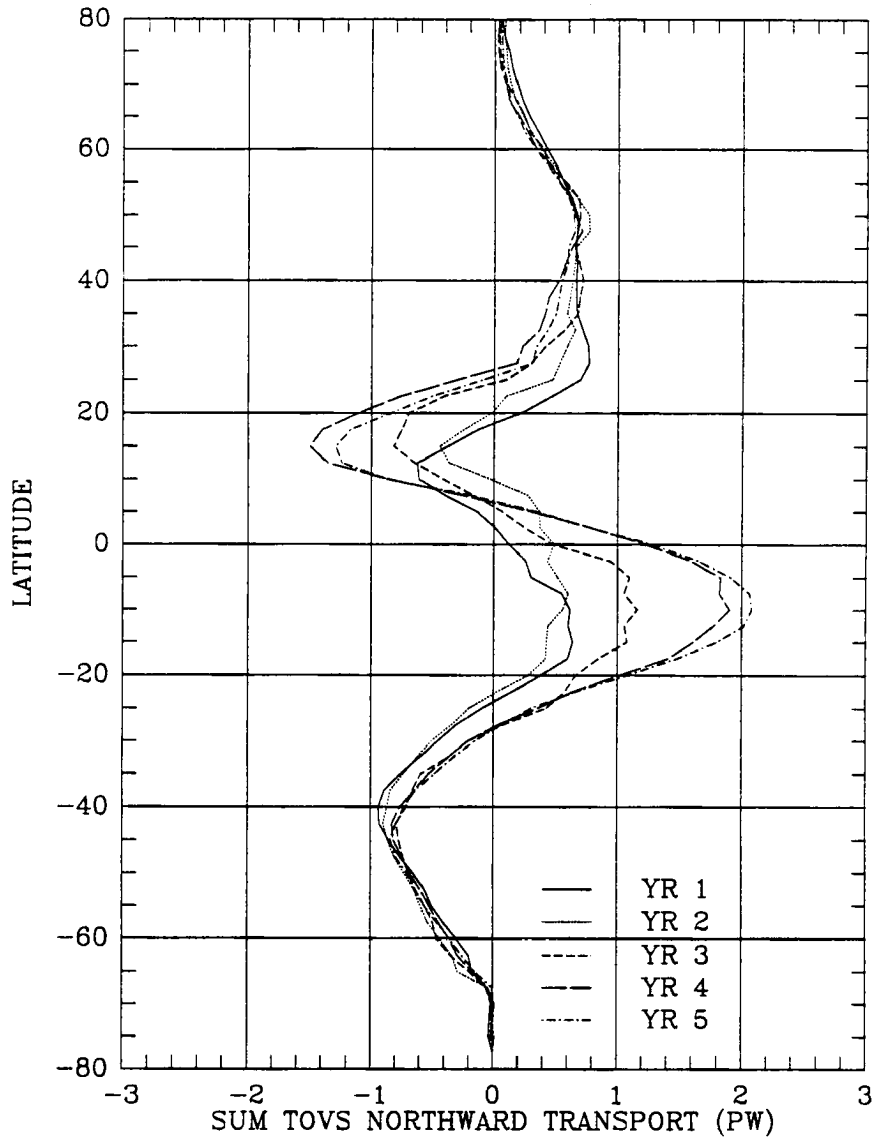

Figure 4.15: Annually averaged total poleward latent heat transport for five individual years using ISCCP TOVS moisture and ECMWF wind data. Units are petawatts.

neglected. Fig. 4.16 gives the five annual precipitation minus evaporation profiles based on water vapor transports using TOVS moisture and ECMWF wind data. Regions where precipitation exceeds evaporation are located near 5N, and poleward of 45 degrees in both hemispheres. Evaporation dominates in the subtropics, where large areas of clear, warm atmosphere promote high sea surface evaporation rates. The larger SH ocean area provides for the maximum difference in net evaporation minus precipitation. Tropical precipitation excesses are the largest, where greatest convergence of low level high moisture values are found.

Since these profiles are based on the annual transport curves, similar problem exist therein. The basic shape of each precipitation minus evaporation curve is a fairly good representation, but few conclusive results may be drawn from them due to the high level of probable error. Actual interannual variations are lost in the noise level, and positions of many features suffer from biased data for the same reasons as given above. In fact, since the TOVS data is stratified within only a few distinct latitude zones, gradients within them would tend to be weak. Therefore, since calculation of net precipitation minus evaporation gives gradient information regarding moisture transport, these gradients are likely to be underestimates as well. See the Appendix for previous independent calculations of this quantity based on primarily land based upper air analyses. It is obvious that much future work is required to better quantify atmospheric moisture content and transport on the large scale.

4.4 CONTRIBUTION OF TOTAL LATENT HEAT TRANSPORT TO THE TOTAL POLEWARD HEAT FLUX

Peak annual poleward heat transport estimates have been made for both oceanic and atmospheric components, as well as their sum. Much uncertainty exists in these estimates, so an alternative method for calculating the total poleward heat flux was presented by Vonder Haar and Oort (1973). Annual satellite based radiation budget measurements at the top of the atmosphere were shown to be directly related to the amount of heat transported within the ocean-atmosphere system (storage is assumed negligible in the annual mean),

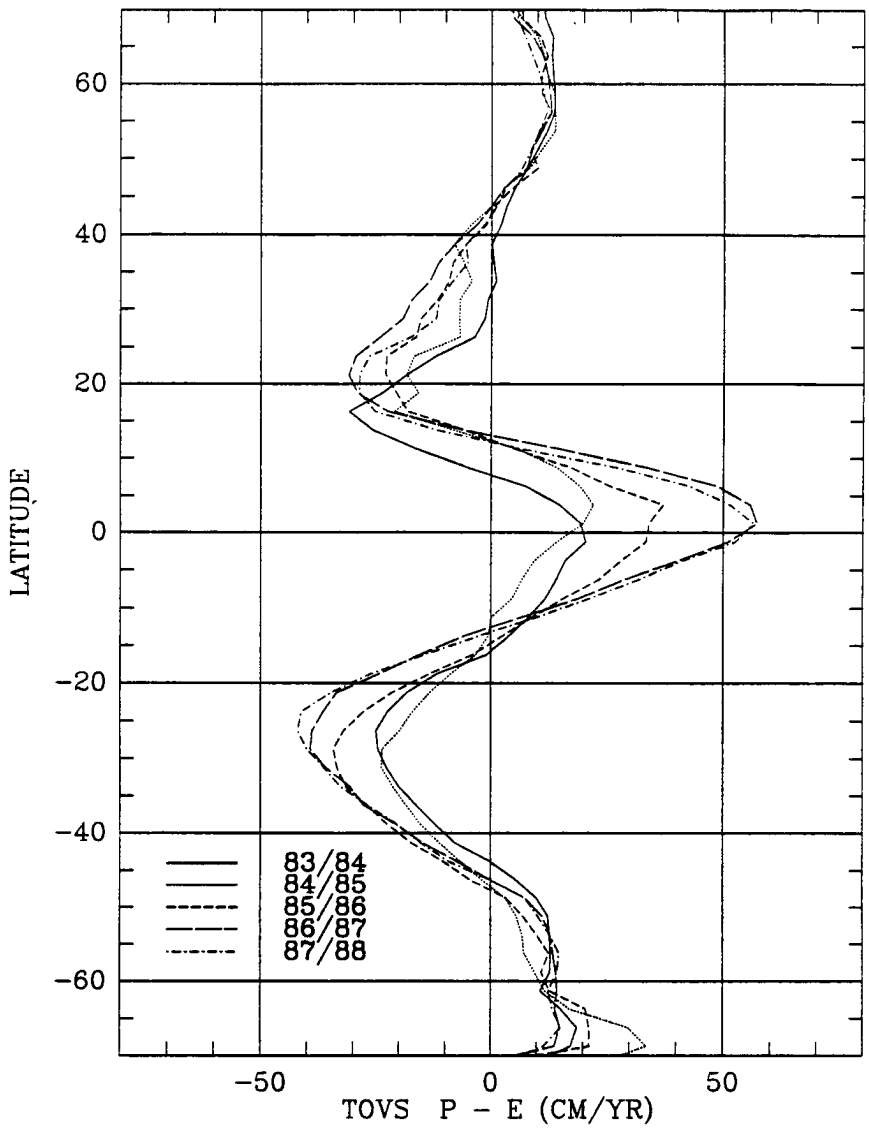

Figure 4.16: Annual net precipitation minus evaporation using five years of ISCCP TOVS transport data.

$$AT + OT + RF = 0 \tag{4.1}$$

where RF is the radiative flux at the top of the atmosphere.

The 1973 study used the radiation observations along with atmospheric heat transport (AT) estimates for the Northern Hemisphere to retrieve the oceanic transport (OT) component as a residual there. A later study by Oort and Vonder Haar (1976) investigated AT, OT, RF, and other quantities using satellite radiation data, and *in situ* atmospheric and oceanic data for the annual cycle. A resent summary of radiation budget and ocean/atmosphere heat flux studies is presented by Vonder Haar (1989). Peak total required AT+OT (near 30N) estimates using the satellite radiation budget method are on the order of 5 PW. The poleward latent heat transport at 30N, as estimated in the present study, is shown to approach 1 PW for the annual averages examined (PLHT estimates given in the Appendix using ECMWF moisture yield values near 2 PW at 30N). It becomes readily apparent that latent heat plays a very important role in moving heat poleward. Vonder Haar and Oort (1973) report a 47 percent oceanic contribution, or 2.25 PW peak transport. If we assume the true 30N peak transport lies somewhere between the estimates given in this study, then at least half of the AT component is likely to due to the latent heat component. Since large uncertainty exists in latent heat transport estimates, it becomes difficult to determine a peak total heat flux value based on the sum of all components. Improved observation from space, as well as from within the atmosphere and oceans, will be key in reducing the uncertainty level of global heat fluxes.

Chapter 5

CONCLUSION

The highly variable nature of atmospheric moisture in both time and space has prevented adequate description of the role of this quantity in climate. Using recently developed global data sets, the present study addresses the problem of characterizing large scale atmospheric moisture distribution and poleward latent heat transport. Three components of the total flux are individually examined, and show very different mechanisms for moving moisture from one latitude belt to an adjacent one. Tropical low level flow consistently feeds the ITCZ, which shows seasonal latitudinal variations. Peak transient eddy transports are during April and October during seasonal transitions. Standing eddies move moisture poleward at subtropical latitudes. In general, the eddy processes move moisture, and latent energy toward the colder, dryer high latitudes, while the mean meridional circulation moves moist energy away from the poles toward the convergence zone.

Analyzed precipitable water content fields show many expected mean features but are limited in detailing important smaller scale phenomena. Large scale phenomena such as tropical convergence zones, areas of minima over elevated terrain, and the maritime continent maximum are all shown clearly. Gradients across continental margins are shown, and variations across various land surface types are apparent.

Model changes during the study period affected annual, and climatological means of both the moisture distribution, and its flux. Inherent problems with the TOVS retrieval scheme prevented the collection of information within totally cloudy areas, and a significant loss of data is attributed to this problem. But, since all these problems are well documented, and their relative magnitudes can be somewhat inferred, new information is gained using the satellite based moisture data.

Moisture plays a critical role in atmospheric processes. In order to further advance our knowledge of its distribution, transport, and interaction with other atmospheric variables such as clouds and radiation, new and improved data sets must be developed. Characterization of global precipitable water content will be improved when long term satellite based microwave data sets are compiled. While not easily applicable over land, the retrieval of total column moisture over ocean is possible in clear and cloudy scenes. Microwave measurements describe important small scale features well, and give more accurate estimates in clear areas than those of present infrared retrieval methods. When coupled with improved analyses of ground based atmospheric soundings over land, improved global analyses will undoubtedly be made.

The future offers to bring much improved satellite based sensing of atmospheric moisture. The next generation polar orbiting program will feature infrared and microwave instruments with higher resolution capability. However, new global data sets based on other future space based sensors are quite a few years off, so we must look to the presently available sources for additional information content. Archived ECMWF analyses are not produced with temporal consistency in mind as they are a product of the short term forecast initialization scheme, and periodic model changes alter the analysis climate. Possible removal of a number of the biases could improve the data set for use in climate applications.

The operational geostationary satellite programs allow for an additional large scale moisture data set. Data coverage is sufficient between 50N and 50S, where much of the important transports occur. The Visible Infrared Spin-Scan Radiometer (VISSR) Atmospheric Sounder (VAS) has multispectral capability (Smith, 1983) and is ideal for the study of transient systems. The geostationary orbit makes constant observation possible, and high frequency temporal variations are easily captured. Future systems, including the geostationary platform, will carry advanced sounding systems and yield important new information on the regional scale.

Merging two or more data sets would yield a superior analysis which then could benefit from the individual strengths of each input field. Also needed are reanalyses of

existing data sets. The present study used only raw (clear air) data, and eliminated filled data areas. Use of this filled data may provide additional insight given that a careful analysis is done. Satellite based soundings are already being regenerated using alternative retrieval methods. The statistical scheme used in the operational TOVS program can be replaced with the more computationally intensive physical schemes, which tend to yield better clear sky moisture profiles. Careful examination of these potential data sources will gradually provide for an improved description of atmospheric moisture, especially in important smaller scale features. Better understanding of moist processes will advance our knowledge of many other atmospheric systems, and aid in our understanding of their interactions.

REFERENCES

Agarwal, V. K., and A. V. Ashajayanthi, 1983: Boundary-layer structure over tropical oceans from TIROS-N infrared sounder observations. *J. Clim. Appl. Meteor.*, **22**, 1305-1311.

Bannon, J. K., and L. P. Steele, 1960: Average water-vapor content of the air. *Geophysical Memoir No. 102*, British Met. Office, London.

Benton, G. S., and M. A. Estoque, 1954: Water-vapor transfer over the North American continent. *J. Meteorol.*, **11**, 462-477.

Budyko, M. I., 1963: *Atlas of the Heat Balance of the Earth* (In Russian.) Moscow, Globnaia Geofiz. Observ., 69 pp.

Carissimo, B. C., A. H. Oort, and T. H. Vonder Haar, 1985: Estimating the meridional energy transports in the atmosphere and ocean. *J. Phys. Oceanogr.*, **15**, 82-91.

Chen, T.-C., 1985: Global water vapor flux and maintenance during FGGE. *Mon. Wea. Rev.*, **113**, 1801-1819.

Colorado State University, 1982: Workshop on Satellite Meteorology. July 19-23, 1982, Ft. Collins, Colorado.

Gruber, A., and C. D. Watkins, 1979: Preliminary evaluation of initial atmospheric moisture from the TIROS-N sounding system. *Satellite Hydrology, Proc. Fifth Ann. Symp. on Remote Sensing*, Minneapolis, Amer. Water Resources Assoc., 115-123.

Illari, L., 1989: The quality of satellite precipitable water content data and their impact on analyzed moisture fields. *Tellus*, **41A**, 319-337.

Kann, D. M., S-K Yang, and A. J. Miller, 1990: Atmospheric energetics and Earth radiation budget. *7th Conf. on Atmospheric Radiation*, San Francisco, Calif. (AMS), J129-J131.

Khalsa, S. J. S., and E. J. Steiner, 1987: Vertical structure in the near-equatorial atmosphere from the TIROS Operational Vertical Sounders (TOVS). *17th Conf. on Hurricanes and Tropical Meteorology*, Miami, Amer. Meteor. Soc., 137-141.

Lauritson, L., G. J. Nelson, and F. W. Porto, 1979: Data Extraction and Calibration of TIROS-N/NOAA Radiometers. *NOAA Tech. Memorandum NESS 107*, U.S. Dept. of Commerce, Washington D.C.

Lönnberg, P., and D. Shaw, 1986: ECMWF Data Assimilation Scientific Documentation. *ECMWF Research Manual 1*, Available from ECMWF, Shinfield Park, Reading, U.K.

Lorenc, A. C., 1981: A global three-dimensional multivariate statistical interpolation scheme. *Mon. Wea. Rev.*, **109**, 701-721.

Lorenz, E. N., 1967: *The Nature and Theory of the General Circulation of the Atmosphere*, WMO Publication No. 218, World Meteorlogical Organization, Geneva, Switzerland, 161 pp.

McGuirk, J. P., A. H. Thompson, and N. R. Smith, 1987: Moisture bursts over the tropical Pacific Ocean. *Mon. Wea. Rev.*, **115**, 787-798.

Machenhauer, B., 1977: On the dynamics of gravity oscillations in a shallow water model, with applications to normal mode initialization. *Contributions to Atmospheric Physics*, **50**, 253-271.

Masuda, K, 1988, Meridional heat transport by the atmosphere and the ocean: analysis of FGGE data. *Tellus*, **40A**, 285-302.

Oort, A. H., 1971: The observed annual cycle in the meridional transport of atmospheric energy. *J. Atmos. Sci.*, **28**, 325-339.

Oort, A. H., and T. H. Vonder Haar, 1976: On the observed annual cycle in the ocean-atmosphere heat balance over the Northern Hemisphere. *J. Phys. Oceanogr.*, **6**, 781-800.

Oort, A. H., 1977: Adequacy of the rawinsonde network for global circulation studies tested through numerical model output. *Mon. Wea. Rev.*, **106**, 174-195.

Oort, A. H., 1983: Global atmospheric circulation statistics, 1958-1973. *NOAA Professional Paper No. 14*, 180 pp. + microfiches.

Pasch, R., and L. Illari: 1985: FGGE moisture analysis and assimilation in the ECMWF system. *ECMWF Tech. Memo No. 110.* Available from ECMWF, Shinfield Park, Reading, U.K.

Peixoto, J. P., D. A. Salstein, and R. D. Rosen, 1981: Intra-annual variation in large scale moisture fields. *J. Geophys. Res.*, **86**, 1255-1264.

Rasmusson, E. M., 1966: Diurnal variations in the summer water vapor transport over North America. *Water Resour. Res.*, **2**, 469-477.

Rosen, R. D., D. A. Salstein, and J. P. Peixoto, 1979: Variability in the annual fields of large-scale atmospheric water vapor transport. *Mon. Wea. Rev.*, **107**, 26-37.

Rossow, W. B., L. C. Garder, P. Lu, and A. Walker, 1988: International Satellite Cloud Climatology Project (ISCCP) Documentation of Cloud Data. Available from NOAA NESDIS, Washington D.C., 77pp.

Rossow, W. B., and B. Kachmar , 1988: International Satellite Cloud Climatology Project (ISCCP) Description of Atmospheric Data Set. Available from NOAA NESDIS, Washington D.C., 30pp.

Schiffer, R. A., and W. B. Rossow, 1983: The International Satellite Cloud Climatology Project (ISCCP) - The first project of the World Climate Research Program. *Bull. Amer. Meteor. Soc.*, **64**, 779-784.

Schiffer, R. A., and W. B. Rossow, 1985: ISCCP global radiance data set: a new resource for climate research. *Bull. Amer. Meteor. Soc.*, **66**, 1498-1505.

Schwalb, A., The TIROS-N/NOAA A-G Satellite Series, *NOAA Technical Memorandum NESS 95*, March 1978, 75 pp., U.S. Dept. of Commerce, Washington D.C.

Sellers, W. D., 1965: *Physical Climatology*. The University of Chicago Press, 272 pp.

Smith, W. L., and H. M. Woolf, 1976: The use of statistical covariance matrices for interpreting satellite sounding radiometer observations. *J. Atmos. Sci.*, **33**, 1127-1140.

Smith, W. L., 1983: The retrieval of atmospheric profiles from VAS geostationary radiance observations. *J. Atmos. Sci.*, **40**, 2025-2035.

Starr, V. P., J. P. Peixoto, and G. C. Lividas, 1958: On the meridional flux of water vapor in the Northern Hemisphere. MIT Dept. of Met., Studies of the Atmos., Gen. Circ. II, Final Report, Dec. 31, 1957, pp 124-144.

Starr, V. P., J. P. Peixoto, and A. R. Crisi, 1965: Hemispheric water balance for the IGY. *Tellus*, **17**, 463-472.

Starr, V. P., J. P. Peixoto, and N. E. Gaut, 1970: Momentum and kinetic energy balance of the atmosphere from five years of hemispheric data. *Tellus*, **22**, 251-274.

Starr, V. P., J. P. Peixoto, and R. G. McKean, 1969: Pole-to-pole moisture conditions for the IGY. *Pure Appl. Geophys.*, **15**, 300-331.

Steiner, E. J., and S. J. S. Khalsa, 1987: Sea surface temperature, low-level moisture, and convection in the tropical Pacific, 1982-1985. *J. Geophys. Res.*, **92**, 14217-14224.

Tjemkes, S. A., and G. L. Stephens, 1990: Space borne observations of precipitable water. Part I: SSM/I observations and algorithm. *J. Geophys. Res.*, Submitted.

Trenberth, K. E., 1981: Seasonal variations in global sea level pressure and the total mass of the atmosphere. *J. Geophys. Res.*, **86**, 5238-5246.

Trenberth, K. E., 1987: Global atmospheric mass, surface pressure, and water vapor variations. *J. Geophys. Res.*, **92**, 14815-14826.

Trenberth, K. E., and J. G. Olson, 1988: ECMWF global analyses 1979-1986: circulation statistics and data evaluation. NCAR Tech. Note 300, 82 pp.

Vonder Haar, T. H., and A. H. Oort, 1973: New estimate of annual poleward energy transport by Northern Hemisphere oceans. *J. Phys. Oceanogr.*, **3**, 169-172.

Vonder Haar, T. H., 1989, The Earth radiation budget, atmospheric and oceanic energy transports. *Proceedings, International Radiation Symposium 1988*, Lille, France, 1988 (IAMAP). A. Deepak Publishing, Hampton, VA.

Werbowetzki, A., 1981: Atmospheric sounding users guide. *NOAA Tech. Rep. NESS 83*, U.S. Dept. of Commerce, Washington D.C.

Williamson, D. L., 1976: Normal mode initialization procedure applied to forecasts with the global shallow-water equations. *Mon. Wea. Rev.*, **104**, 195-206.

Appendix A

ADDITIONAL ESTIMATES OF PRECIPITABLE WATER CONTENT, LATENT HEAT TRANSPORT, AND NET PRECIPITATION MINUS EVAPORATION

To complement the TOVS moisture and ECMWF wind fields, additional data is examined for further insight. ECMWF moisture data is analyzed (as PWC fields) and paired with the model winds for transport calculations. An independent estimate of PWC for one month using microwave data provides new information not seen in the TOVS data. Transport comparisons are done using a previous ground based study (see Oort, 1971), and transports made with TOVS and ECMWF moisture data. Finally, precipitation minus evaporation profiles are compared with some early estimates by Budyko (1963) and Starr *et al.* (1969).

A.1 PRECIPITABLE WATER CONTENT ANALYSES

Moisture fields derived from ECMWF relative humidity (RH) data show similar mean state properties as found in TOVS analyses, while other features are significantly different. A five year timeseries of ECMWF precipitable water content, as shown in Fig. A.1, is very similar to the TOVS PWC timeseries (see Fig.4.5 in the main text). While the ECMWF monthly values are larger, the difference is fairly constant. In fact, the amplitudes of both hemispheric annual cycles are very consistent with the TOVS data. Only the first two NH annual cycles have significantly larger range. A slight drying trend, due to model adjustments for overestimated moisture content, brings the ECMWF annual means closer to the TOVS means. An adjustment of -0.2 centimeters causes the ECMWF curves to nearly match the TOVS curves. Variations within an annual cycle, and even interannual variations are somewhat duplicated during the final three years. This is encouraging, since

the two data sets are essentially independent. (While TOVS soundings have been used in ECMWF humidity analyses since 1985, their effect is small. Only the model tropical rainfall estimates have shown improvement since the TOVS data inclusion.)

The effects of model changes are readily apparent in the annual zonally averaged ECMWF PWC, as displayed in Fig. A.2. Tropical values are largest during 1983-85, while the 1985-86 year showed a minimum. The two succeeding data years showed gradual increases. While annual tropical moisture content is very sensitive to, and is dominated by model changes, PWC in midlatitudes remains more constant. Evidence of overestimation is also seen in global fields of monthly, and annual averages, as given in Figures A.3,A.4 and A.5. Values over elevated land, such as the Tibetan plateau, the western U.S., and the central African highlands, all are much too high in all time means. The ECMWF spectral model had difficulty in properly representing topography at the provided resolution. General features and gradients are comparable, though, with the TOVS fields.

A third analysis of large scale PWC, using satellite microwave data over oceans, shows features not seen in the the ECMWF or TOVS analyses. The Defense Meteorological Satellite Program (DMSP) Special Sensor Microwave / Imager (SSM/I) data set prepared by Tjemkes and Stephens (1990) for September 1987 shows high frequency variations not seen in other data sets (see Fig. A.6). While, once again, mean features are similar to those seen in other data sets, it is the smaller scale ones which are quite different./ One particular feature worth noting lies to the west of the U.S., over the northwest Pacific Ocean. Persistent low-level high pressure for much of the month forced a large amount of tropical moisture northward to nearly 45N. This shows up well in the standard deviation field seen in Figure A.7 (the comparable TOVS standard deviation field is not shown as no real information is contained therein). Features such as these are very important in the general circulation, and must be accounted for to properly characterize the moisture and its flux.

A.2 ANALYSES OF LATENT HEAT TRANSPORT

The model analyzed ECMWF moisture fields, used with the ECMWF winds, are shown to give improved moisture (or latent heat) transport estimates in midlatitudes.

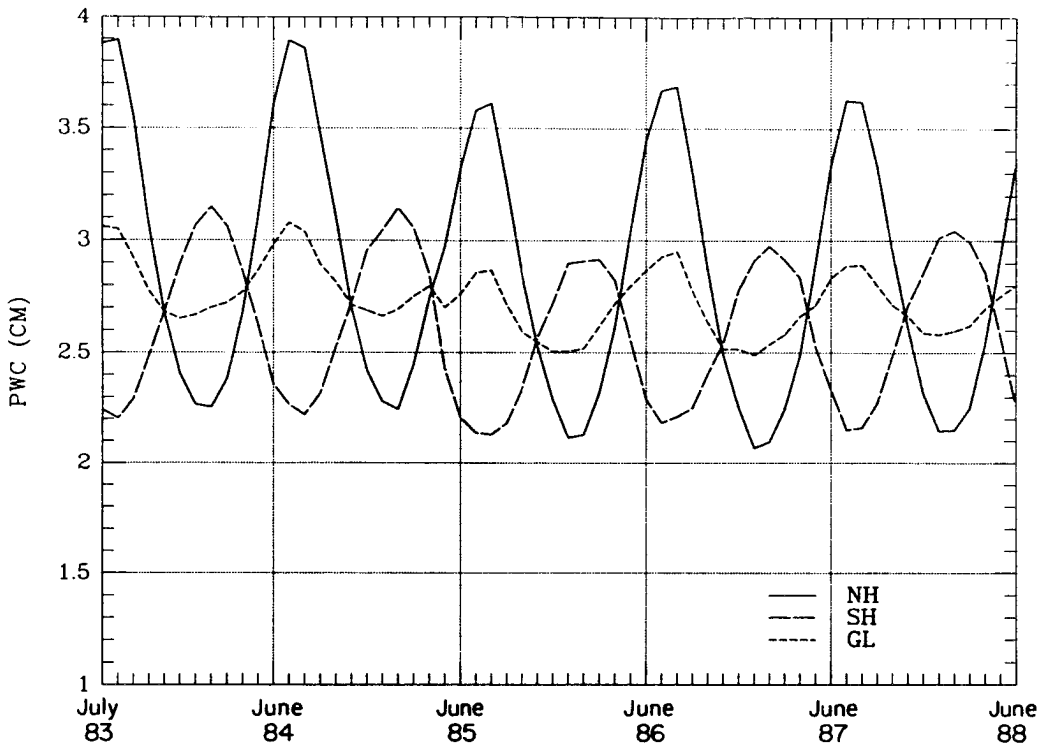

Figure A.1: Time series of hemispheric and globally averaged ECMWF precipitable water content during the five year study period.

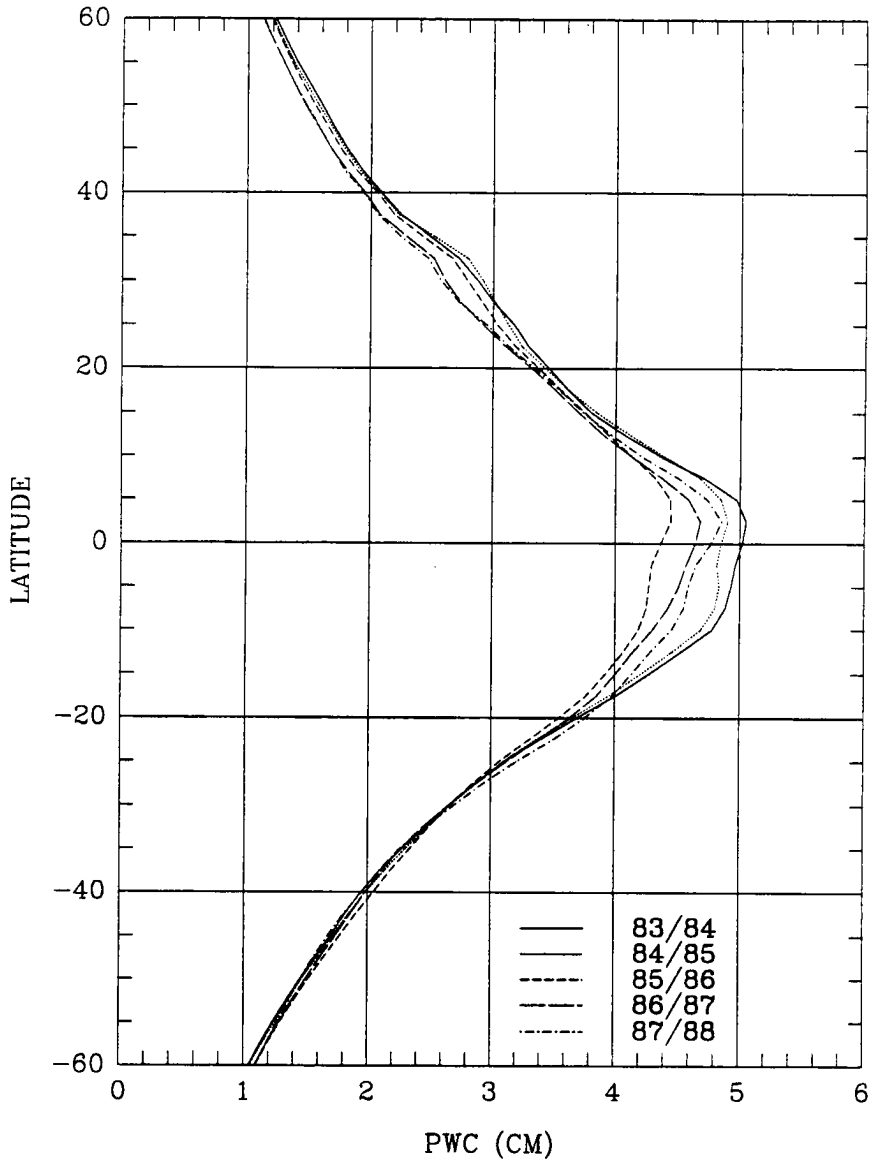

Figure A.2: Annual zonal averages of ECMWF analyzed precipitable water content. Each annual average represents July through the following June.

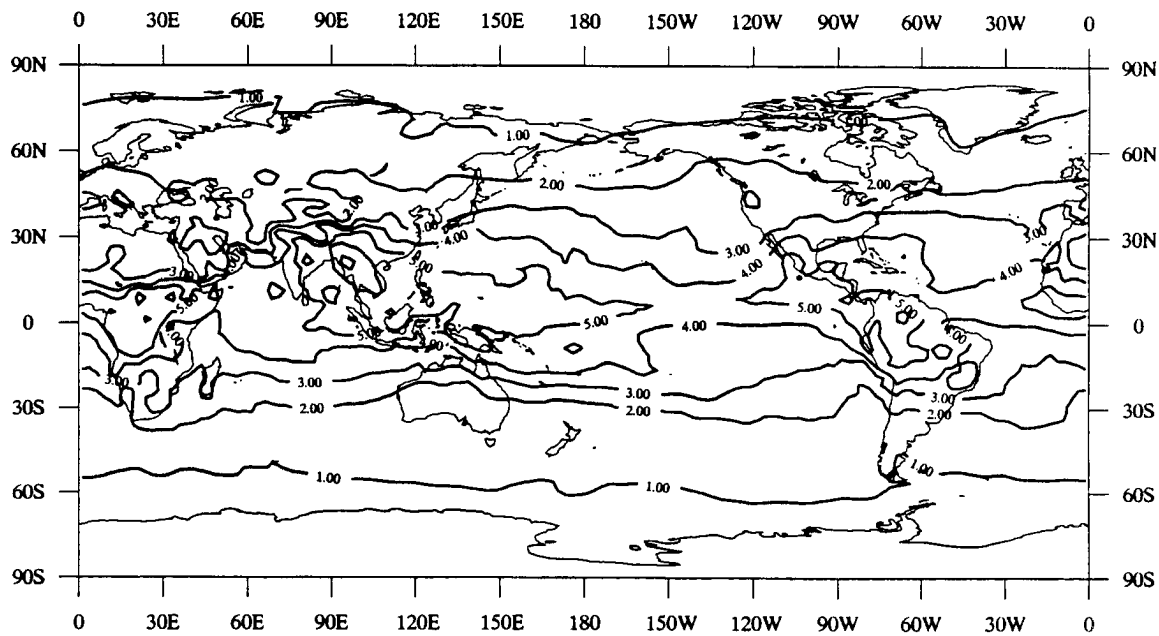

Figure A.3: Monthly average of ECMWF precipitable water content for September, 1987.

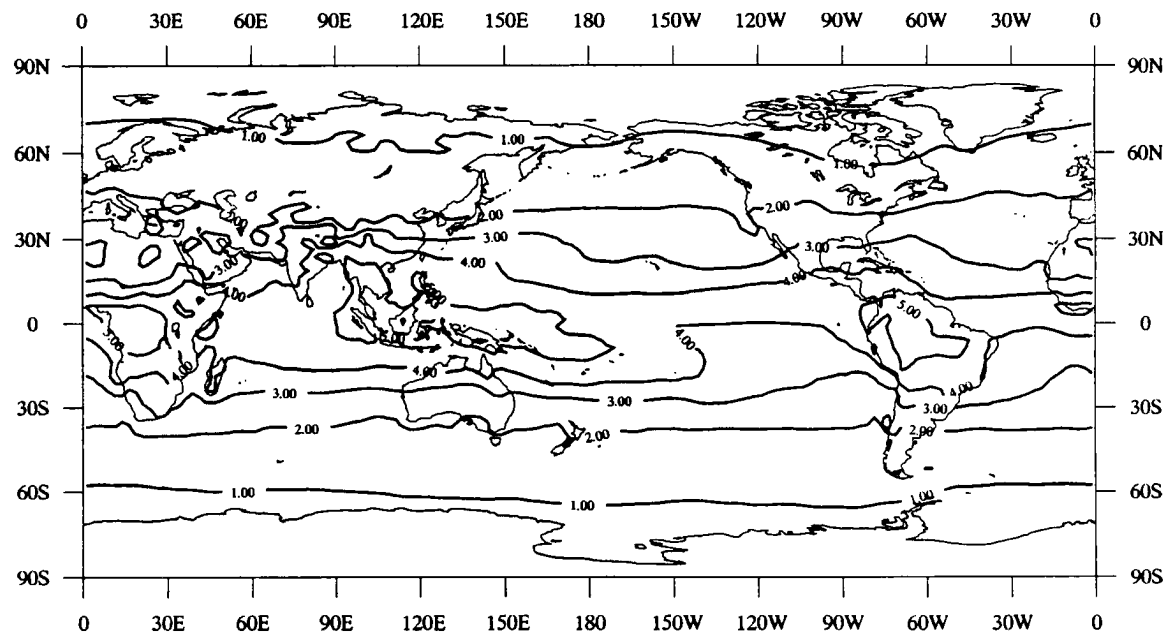

Figure A.4: Annual average of ECMWF precipitable water content for the year beginning on July 1, 1987.

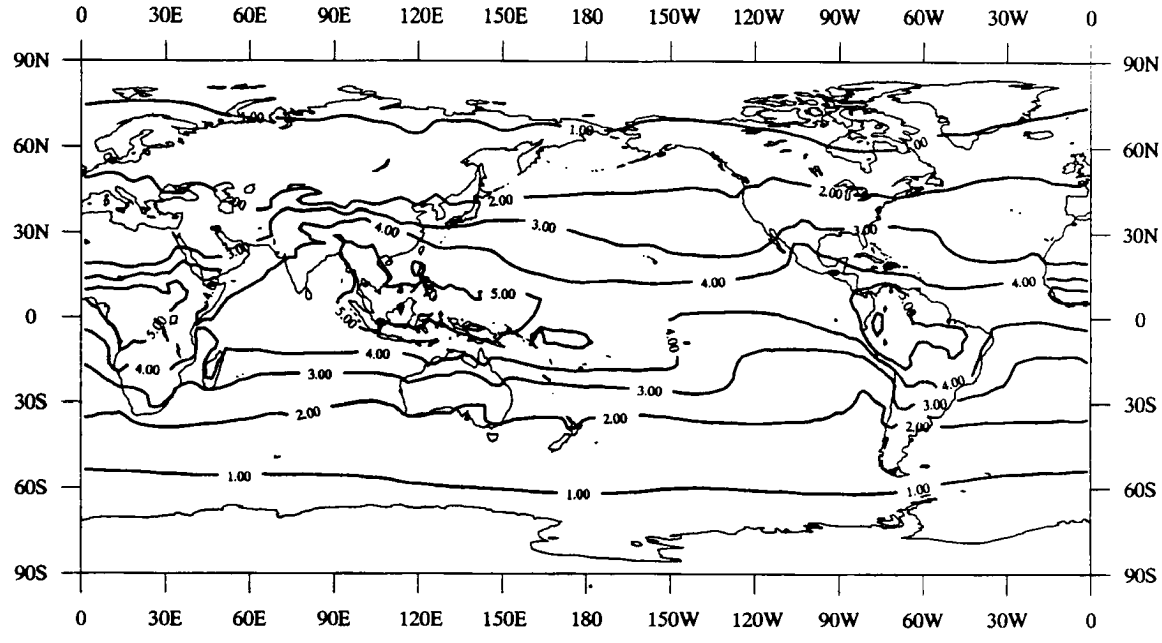

Figure A.5: Mean ECMWF precipitable water content for the five year period of July 1, 1983 through June 30, 1988.

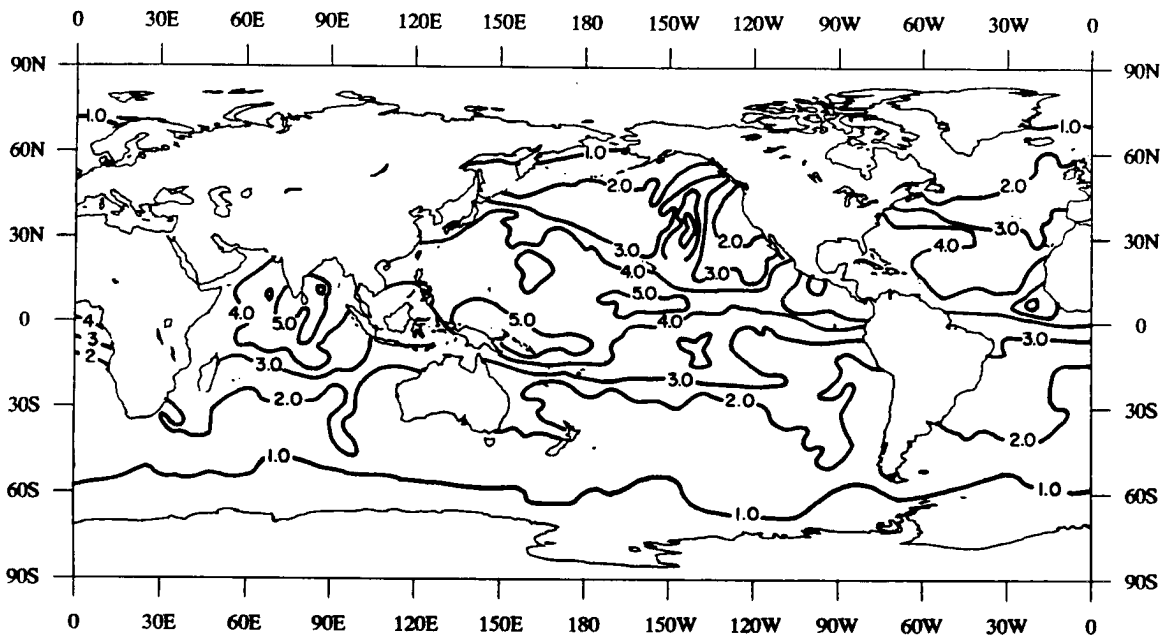

Figure A.6: Monthly mean SSM/I precipitable water content analysis over ocean for September, 1987.

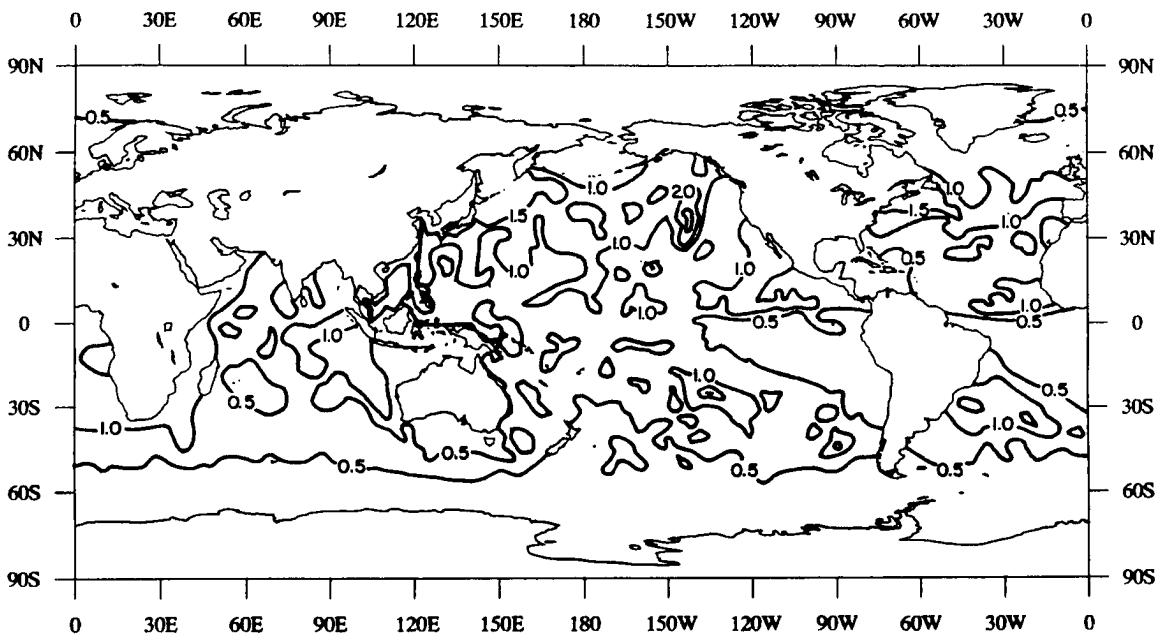

Figure A.7: Standard deviation about the September, 1987 SSM/I precipitable water content monthly mean.

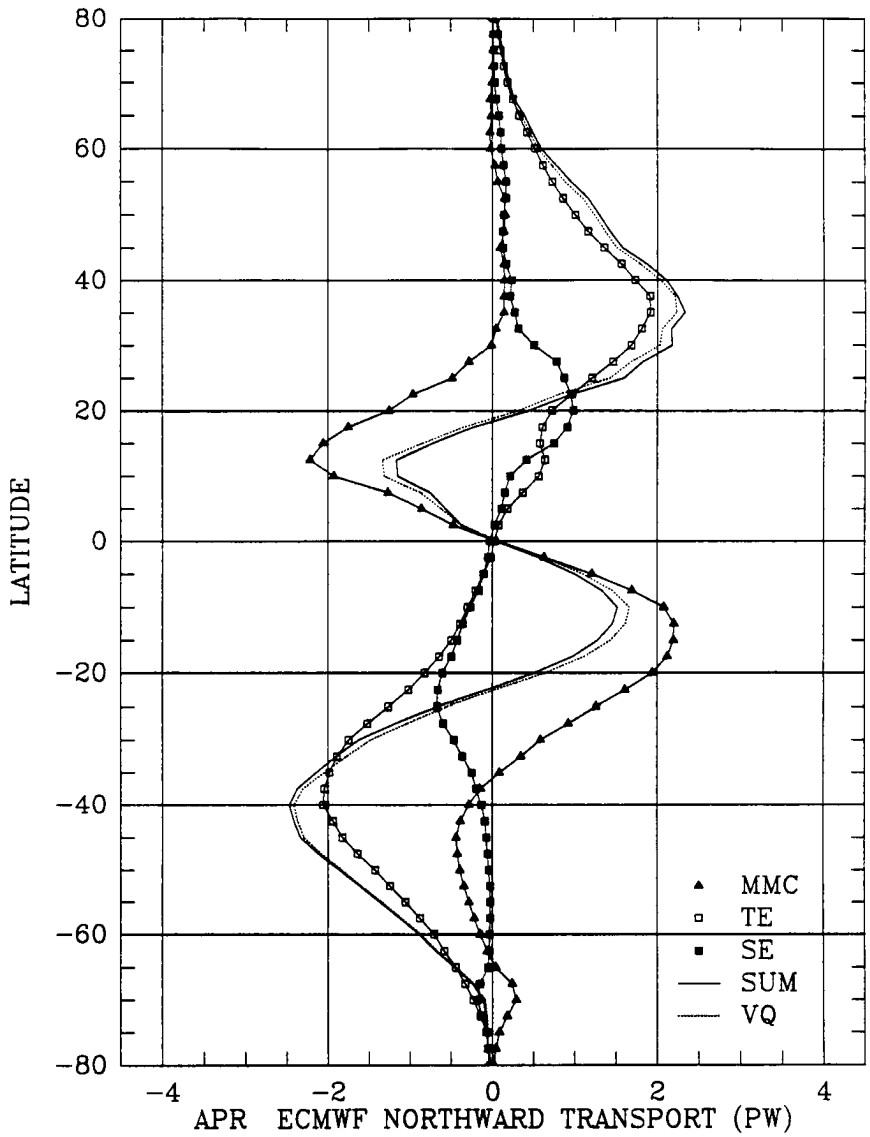

Figure A.9: Northward latent heat transport of the mean meridional circulation (MMC), transport by transient eddies (TE), standing eddies (SE), and the total transport (SUM) based on ECMWF moisture and wind fields for the average of five April months from 1984 to 1988. The computed total transport is labeled VQ. Units are petawatts.

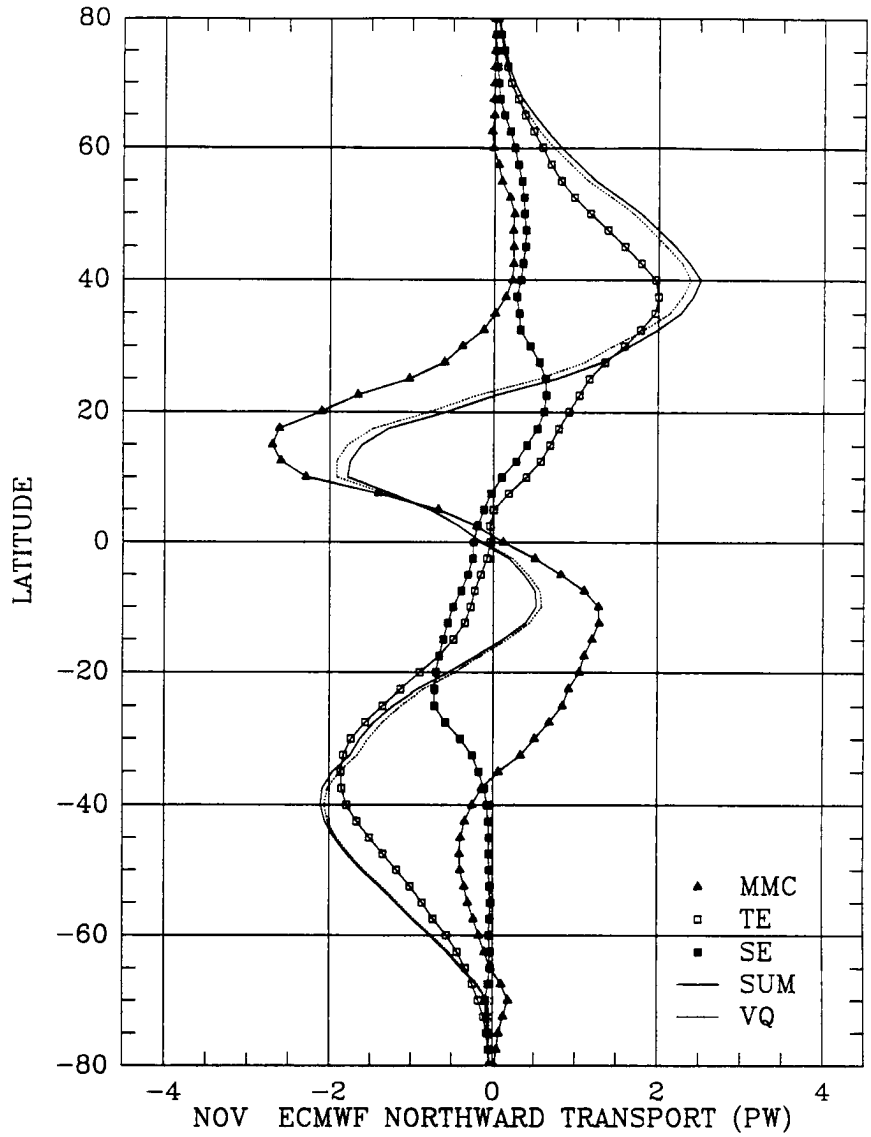

Figure A.10: Northward latent heat transport of the mean meridional circulation (MMC), transport by transient eddies (TE), standing eddies (SE), and the total transport (SUM) based on ECMWF moisture and wind fields for the average of five November months from 1983 to 1987. The computed total transport is labeled VQ. Units are petawatts.

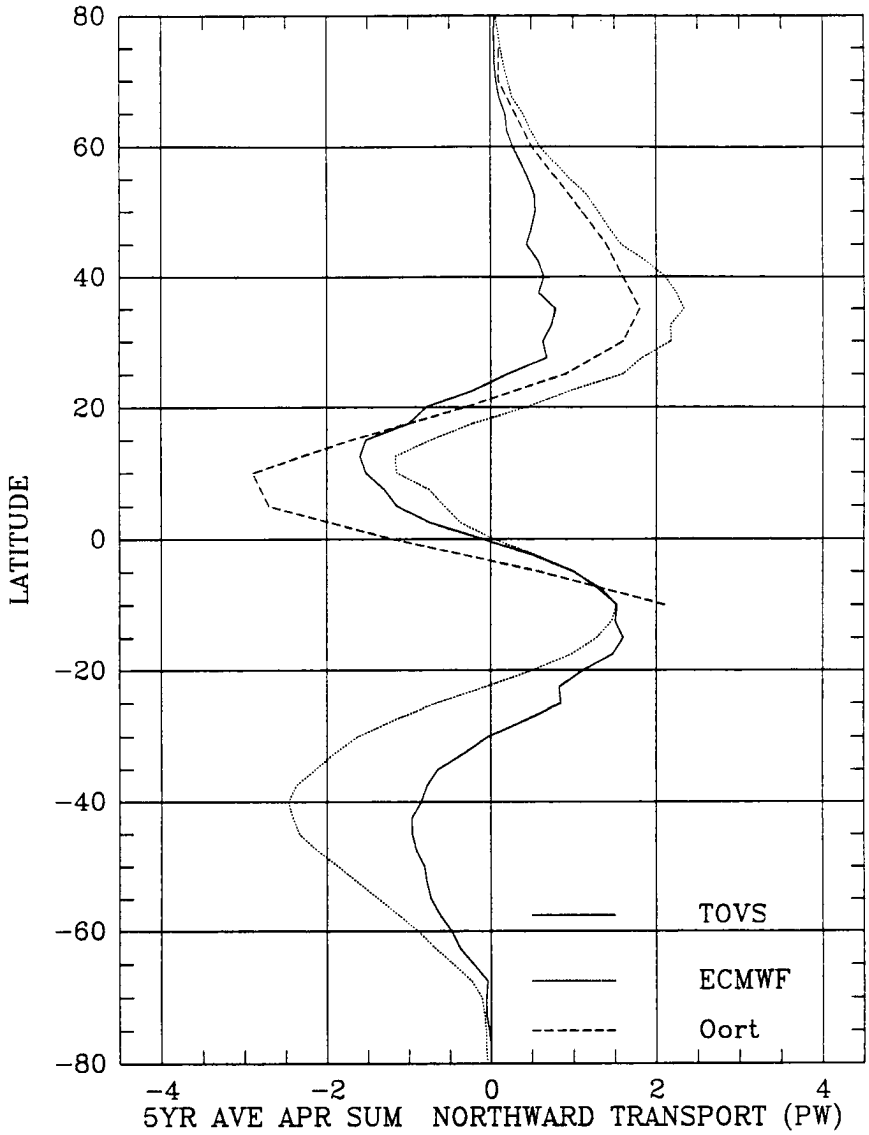

Figure A.13: Northward transport of total latent heat for an average of five April months of ECMWF and TOVS moisture data. A different time period was used by Oort (1971). Units are petawatts.

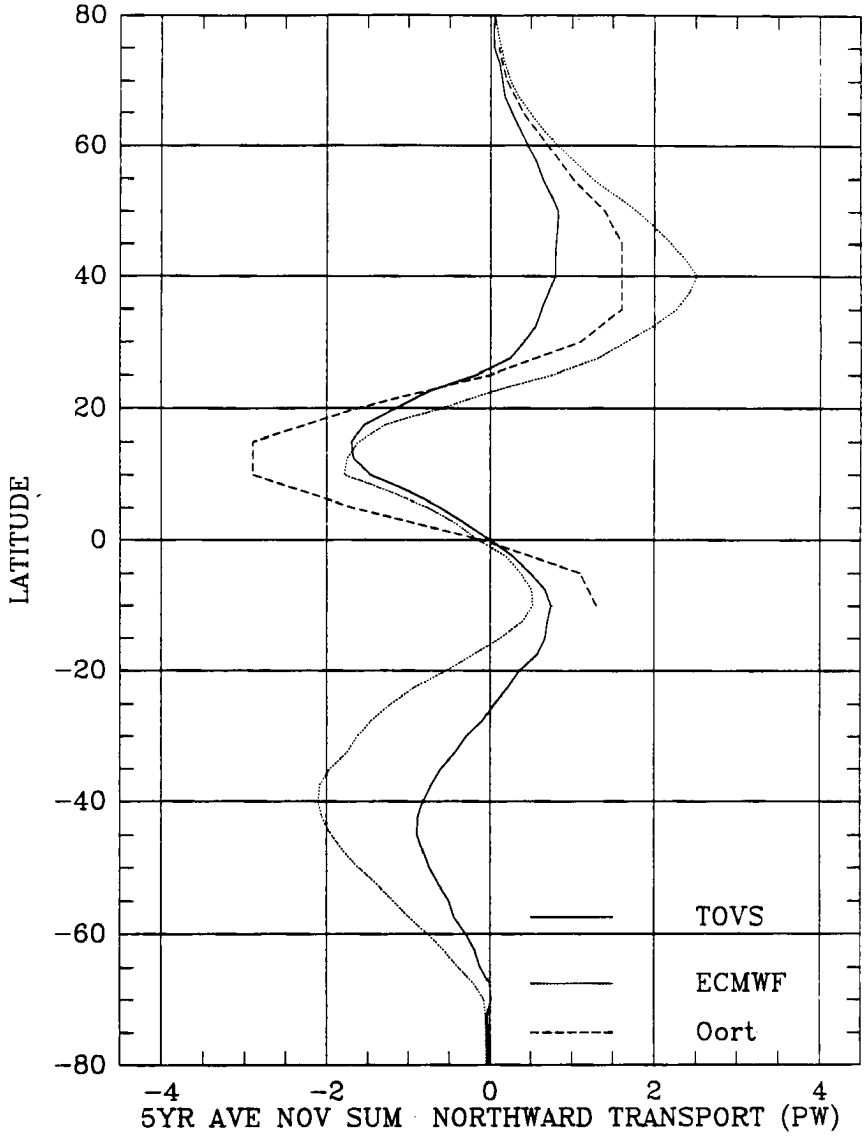

Figure A.14: Northward transport of total latent heat for an average of five November months based on ECMWF and TOVS moisture data. A different time period was used by Oort (1971). Units are petawatts.

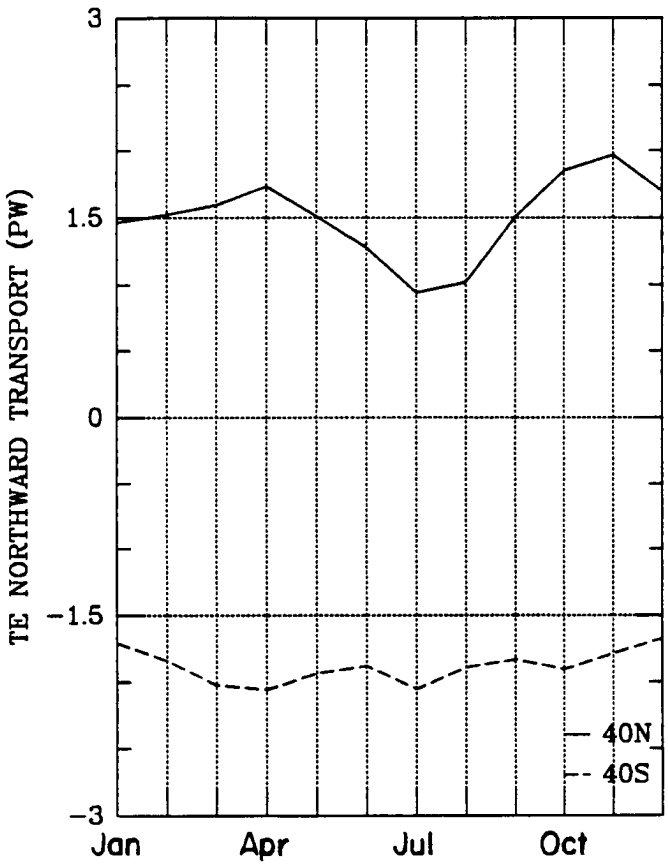

Figure A.11: Annual cycle of latitudinal peak transient eddy latent heat transport based on ECMWF moisture and wind data. Units are petawatts.

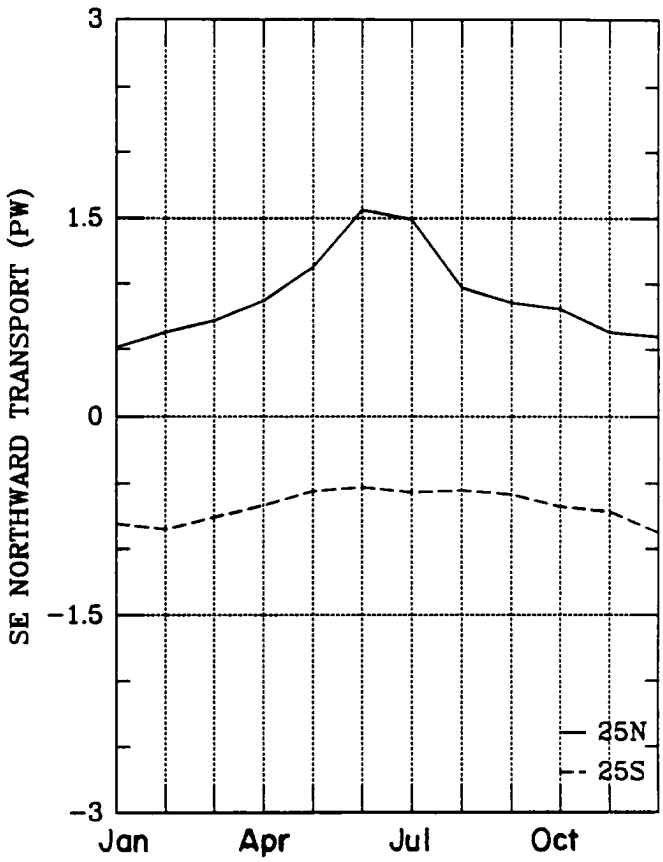

Figure A.12: Annual cycle of latitudinal peak standing eddy latent heat transport based on ECMWF moisture and wind data. Units are petawatts.

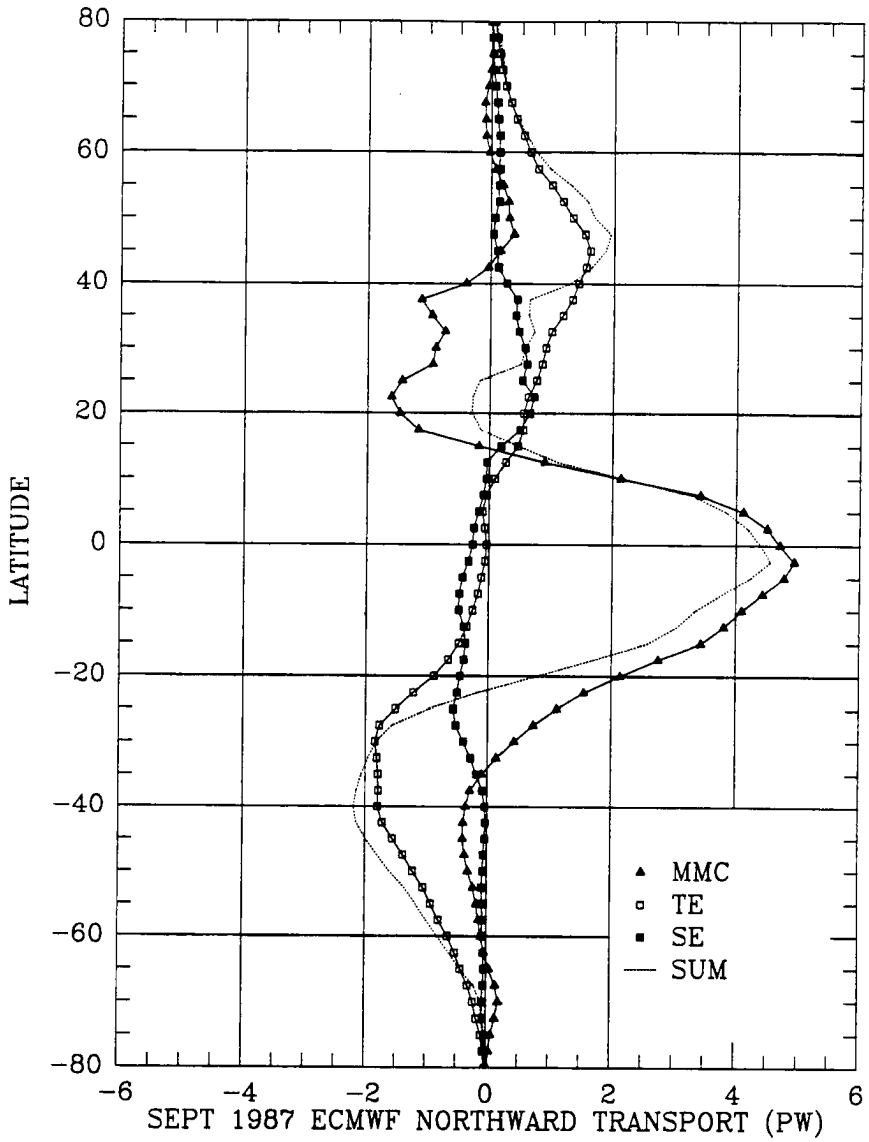

Figure A.8: September, 1987 northward latent heat transport of the mean meridional circulation (MMC), transport by transient eddies (TE), standing eddies (SE), and the total transport (SUM) based on ECMWF moisture and wind fields.

An example for a particular month is shown in Fig. A.8. The September 1987 case has transient eddy transport peaks in excess of 1.75 PW. This is dramatically larger than those in the comparable TOVS monthly average. In fact, all ECMWF components are inflated. The five year composite April and November transport curves, as seen in Figs. A.9 and A.10, show TOVS-like patterns but have much higher amplitude. (The curve labeled "VQ" is the total transport calculated directly, and when compared to the sum of the three components gives an estimate of computational error.)

Increased amplitude is seen in the eddy transport annual cycle (see Figures A.11 and A.12) when compared to the TOVS transports. Higher NH peak average November transient eddy values are near 2 PW while the standing eddy maximum is 1.5 PW in March. The April and November TE peaks in the Northern Hemisphere coincide very well with Oort (1971). The five year averaged April and November SUM transports are compared to this independent estimate (Oort, 1971) in Figs. A.13 and A.14. Oort's data lies between the SUM transports based on TOVS and ECMWF moisture data at midlatitudes during both months. Based on the knowledge of biases within the presently used data sets, it appears the true transport curve lies somewhere near that of Oort, and between the other two. Tropical transport as shown by the Oort curves is largest, due to the differently analyzed wind fields.

Three examples of ECMWF-based annual latent heat transport are shown in Figures A.15, A.16 and A.17. Midlatitude transports are large in these annual means, and reflect the additive nature transport here throughout the year. While monthly transports in the tropics are high, as seen above, the annual values are lower. This result confirms those using TOVS moisture. Model changes are responsible, however, for the increase with time of annual total transport to maximum levels in the final study year of 1987-88. As expected, total interannual transport, as shown in Fig. A.18, and the net annual precipitation minus evaporation (Fig. A.19) have very similar shapes as those based on TOVS moisture, and only magnitude differences exist. When compared to early estimates, ones given here compare favorably, as shown in Fig. A.20.

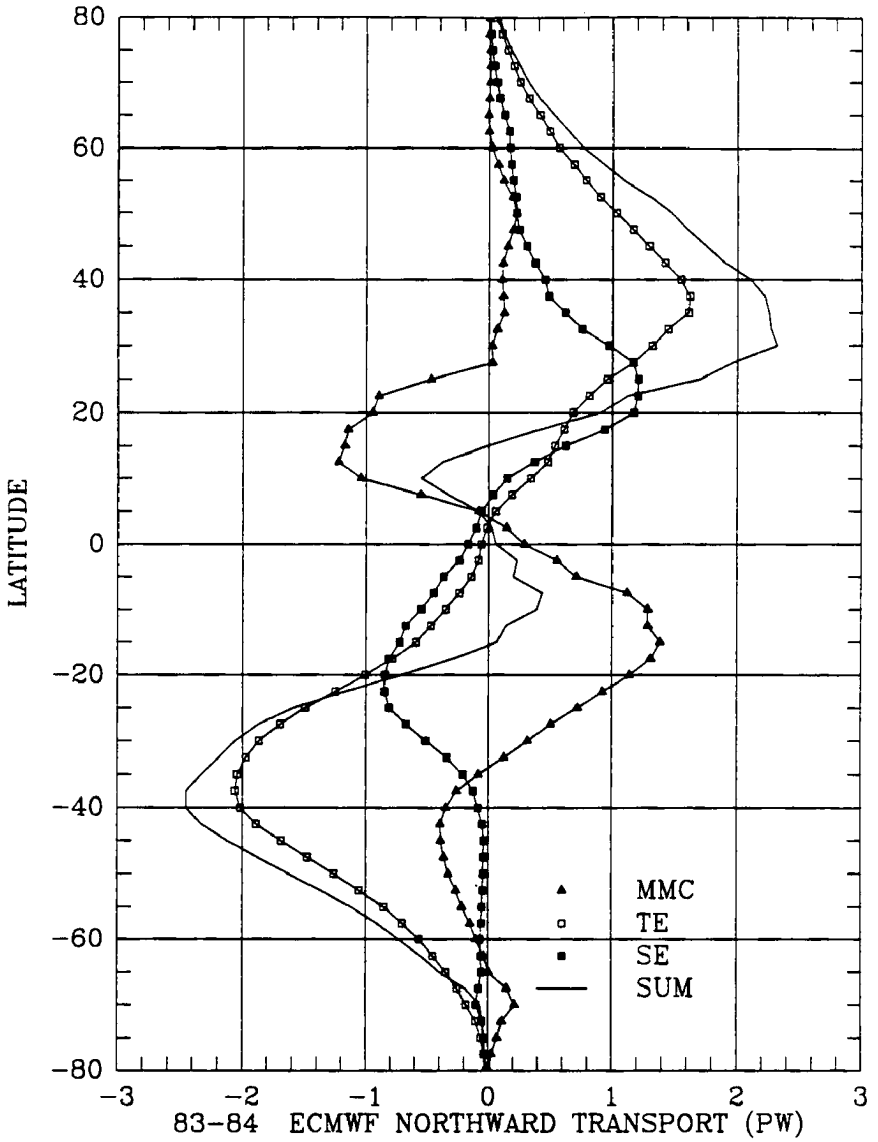

Figure A.15: Annual average of the northward latent heat transport of the mean meridional circulation (MMC), transport by transient eddies (TE), standing eddies (SE), and the total transport (SUM) based on ECMWF moisture and wind fields for the year beginning on July 1, 1983. Units are petawatts.

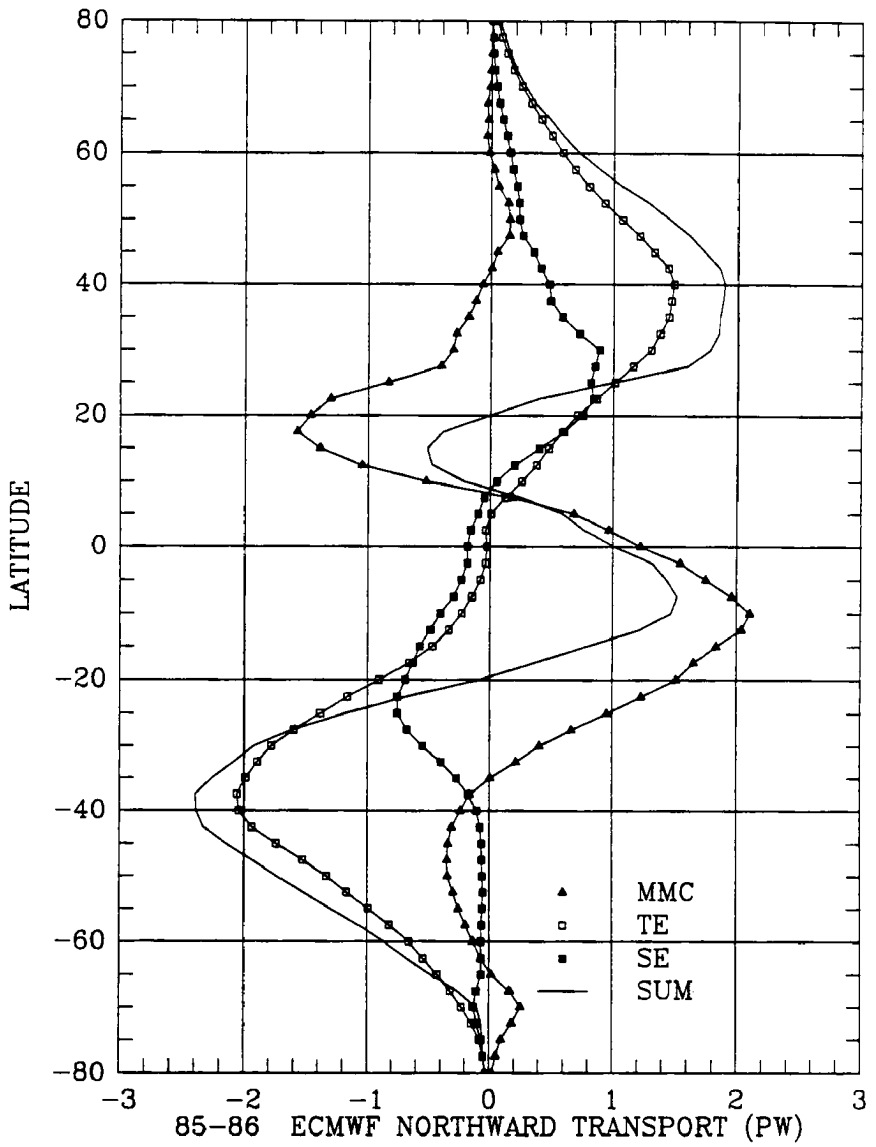

Figure A.16: Annual average of the northward latent heat transport of the mean meridional circulation (MMC), transport by transient eddies (TE), standing eddies (SE), and the total transport (SUM) based on ECMWF moisture and wind fields for the year beginning on July 1, 1985. Units are petawatts.

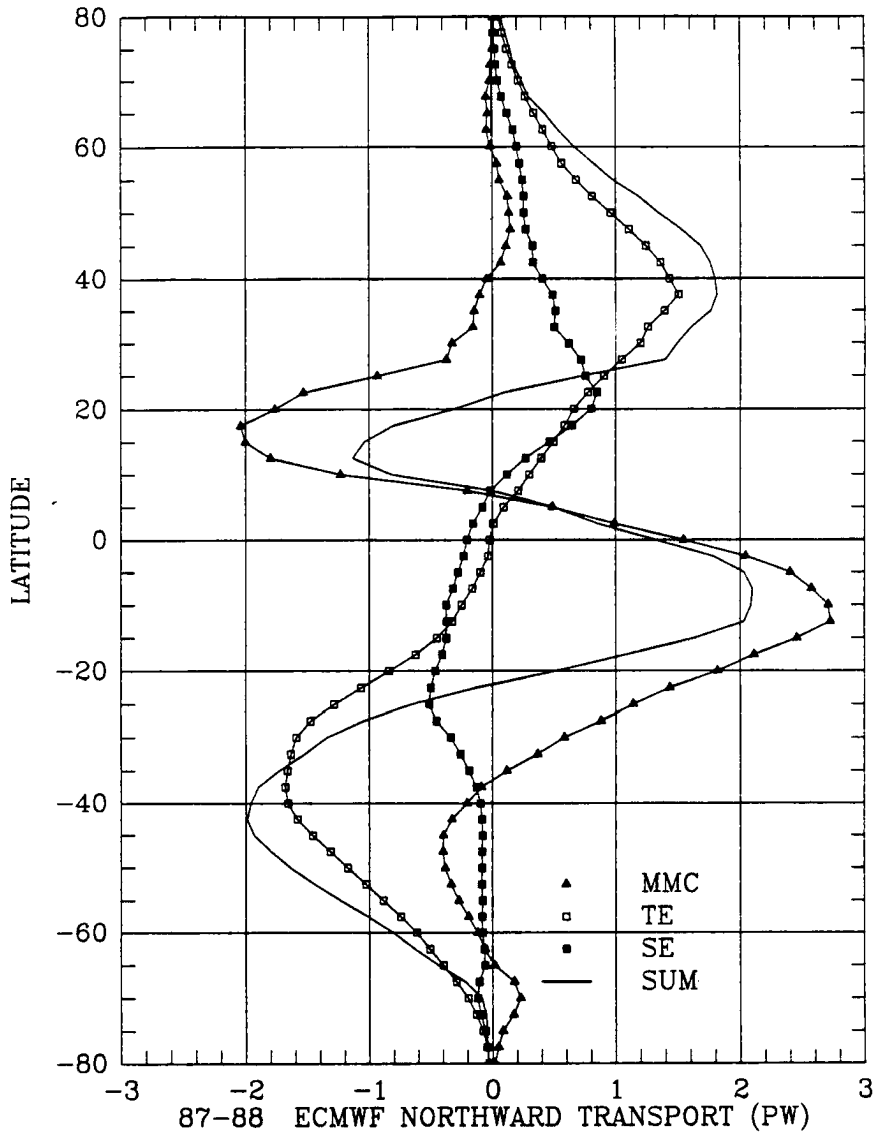

Figure A.17: Annual average of the northward latent heat transport of the mean meridional circulation (MMC), transport by transient eddies (TE), standing eddies (SE), and the total transport (SUM) based on ECMWF moisture and wind fields for the year beginning on July 1, 1987. Units are petawatts.

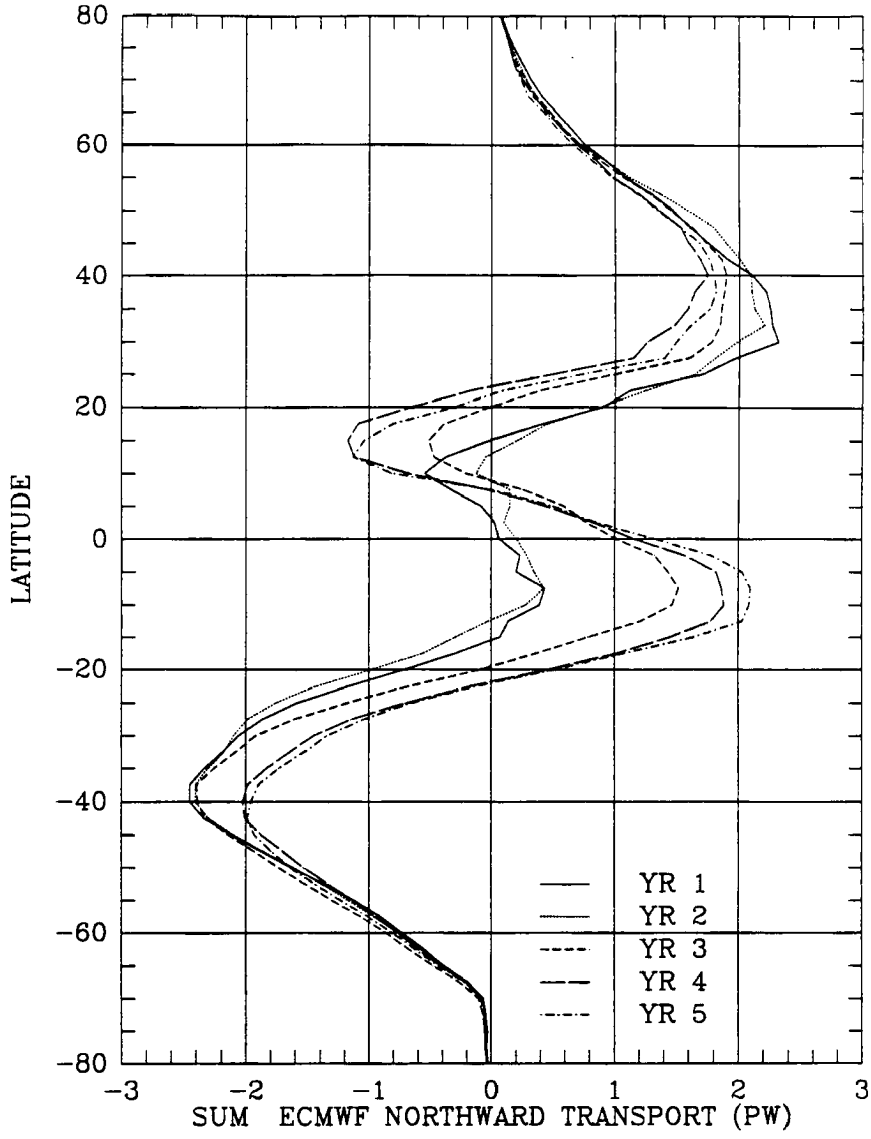

Figure A.18: Annually averaged total poleward latent heat transport for five individual years of ECMWF data. Units are petawatts.

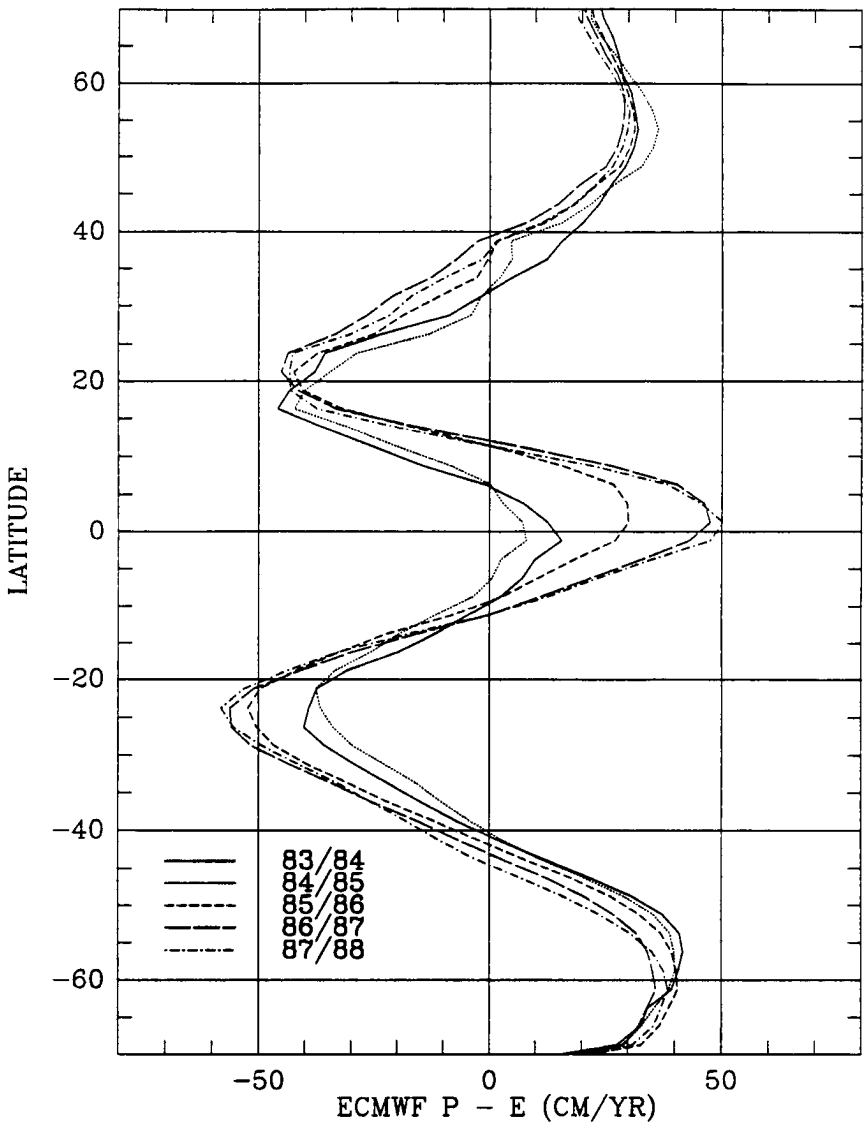

Figure A.19: Annual net precipitation minus evaporation using five years of ECMWF data.

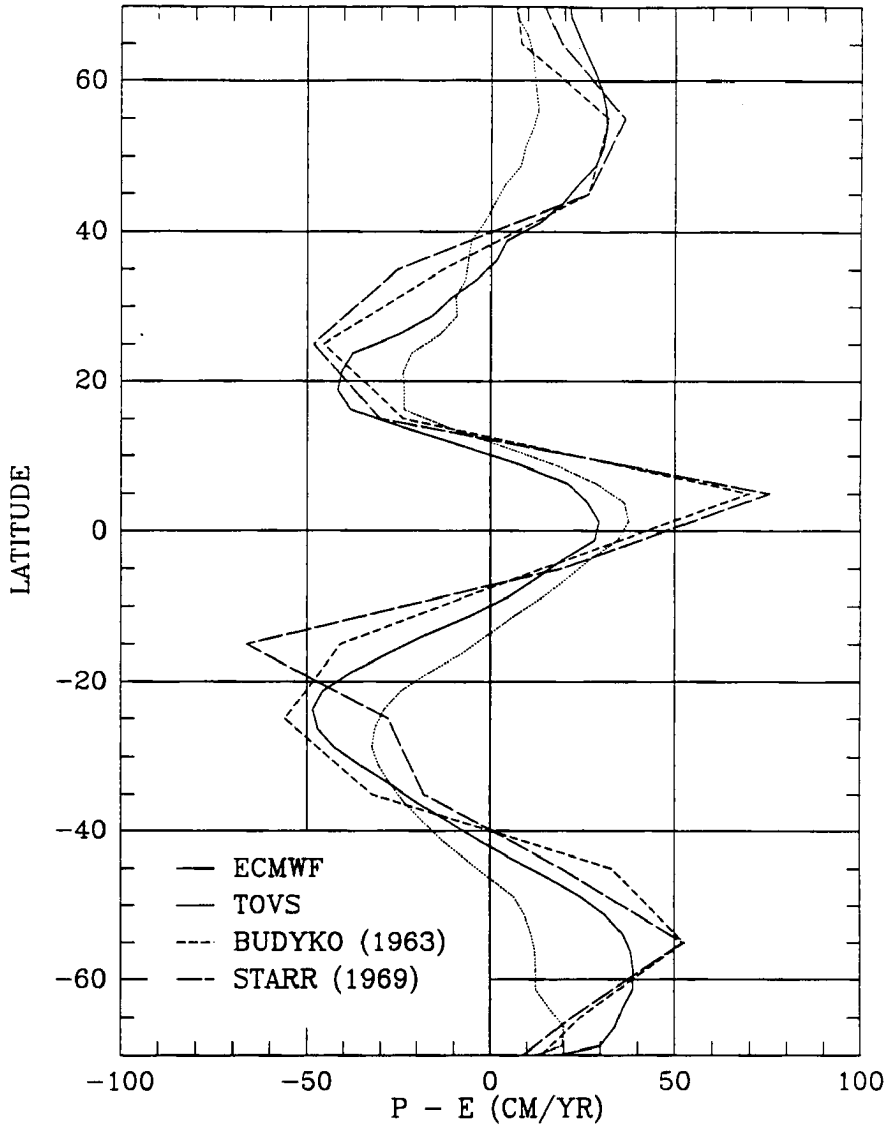

Figure A.20: Various estimates of annual net precipitation minus evaporation.